haematologica
Journal of the Ferrata Storti Foundation

Reduced GATA1 levels are associated with ineffective erythropoiesis in sickle cell anemia

by Sara El Hoss, Panicos Shangaris, John Brewin, Maria Eleni Psychogyiou, Cecilia Ng, Lauren Pedler, Helen Rooks, Érica M.F. Gotardo, Lucas F.S. Gushiken, Pâmela L. Brito, Kypros H. Nicolaides, Nicola Conran, David C. Rees, and John Strouboulis

Received: June 4, 2024.
Accepted: November 27, 2024.

Citation: Sara El Hoss, Panicos Shangaris, John Brewin, Maria Eleni Psychogyiou, Cecilia Ng, Lauren Pedler, Helen Rooks, Érica M.F. Gotardo, Lucas F.S. Gushiken, Pâmela L. Brito, Kypros H. Nicolaides, Nicola Conran, David C. Rees, and John Strouboulis. Reduced GATA1 levels are associated with ineffective erythropoiesis in sickle cell anemia. Haematologica. 2024 Dec 5. doi: 10.3324/haematol.2024.286010 [Epub ahead of print]

Publisher's Disclaimer.
E-publishing ahead of print is increasingly important for the rapid dissemination of science. Haematologica is, therefore, E-publishing PDF files of an early version of manuscripts that have completed a regular peer review and have been accepted for publication.
E-publishing of this PDF file has been approved by the authors.
After having E-published Ahead of Print, manuscripts will then undergo technical and English editing, typesetting, proof correction and be presented for the authors' final approval; the final version of the manuscript will then appear in a regular issue of the journal.
All legal disclaimers that apply to the journal also pertain to this production process.

Reduced GATA1 levels are associated with ineffective erythropoiesis in sickle cell anemia

Running title: Reduced GATA1 in SCA erythropoiesis

Sara El Hoss[1*], Panicos Shangaris[2,3,4#], John Brewin[1,5#], Maria Eleni Psychogyiou[1], Cecilia Ng[1], Lauren Pedler[1], Helen Rooks[1], Érica M. F. Gotardo[6], Lucas F. S. Gushiken[6], Pâmela L. Brito[6], Kypros H Nicolaides[2,4], Nicola Conran[6], David C. Rees[1,5], John Strouboulis[1*]

[1] Red Cell Haematology Lab, Comprehensive Cancer Centre, School of Cancer and Pharmaceutical Sciences, King's College London, United Kingdom

[2] Women and Children's Health, School of Life Course & Population Sciences, King's College London, London, United Kingdom

[3]Peter Gorer Department of Immunobiology, School of Immunology & Microbial Sciences, Faculty of Life Sciences & Medicine, King's College London, London, United Kingdom

[4] Harris Birthright Research Centre for Fetal Medicine, King's College Hospital, London, United Kingdom

[5] Department of Haematological Medicine, King's College Hospital, London, United Kingdom,

[6] Hematology and Transfusion Center, Universidade Estadual de Campinas (UNICAMP), Campinas - São Paulo, Brazil

*Corresponding author #equal contribution

Corresponding Author: Dr Sara El Hoss, sara.el-hoss@institutimagine.org

Pr John Strouboulis, john.strouboulis@kcl.ac.uk

Acknowledgements

We sincerely thank the King's College London, Biological Services Unit, the Advanced Cytometry Platform, R&D Department, Guy's and St Thomas' NHS Foundation Trust, Guy's Hospital, London SE1 9RT and the Central Diagnostic Services at The Queen's Veterinary School Hospital, University of Cambridge for the support with this project. We would like to thank Dr Carlo Scala (King's College London) and Dr Arnaud Chêne (INSERM) for their support. We would also like to sincerely thank Dr Julien Gernier and Dr Wassim El Nemer (Etablissement Français du Sang) for their support.

Funding

SEH received funding from the European Union's Horizon 2020 Research and Innovation Programme under the Marie Sklodowska-Curie grant agreement number 101024970. Part of this study was funded by the Fetal Medicine Foundation (PS & KN) (registered charity 1037116), and supported by the National Institute for Health Research (NIHR) Biomedical Research Centre at Guy's and St Thomas' National Health Service Foundation Trust and King's College London (IS-BRC-1215–20006).

Authorship Contributions

SEH designed the research study, designed, and conducted experiments, analyzed data, wrote and edited the manuscript. PS designed and conducted experiments, analyzed data, and edited the manuscript. JB provided biological samples, discussed data, and edited the manuscript. MEP, CN, LP, HR, EG, LG and PB conducted experiments and acquired data. KN discussed data and edited the manuscript. NC designed experiments analyzed data and edited the manuscript. DR participated to the design of the research, discussed data, and edited the manuscript. JS designed the study, discussed data and edited the manuscript.

Disclosure of Conflicts of Interest

The authors declare no conflict of interest.

Data Sharing Statement

The data supporting the findings of this study are available from the corresponding author upon reasonable request.

Abstract:

Ineffective erythropoiesis (IE) is defined as the abnormal differentiation and excessive destruction of erythroblasts in the marrow, accompanied by an expanded progenitor compartment and relative reduction in the production of reticulocytes. It is a defining feature of many types of anemia, including beta-thalassemia. GATA1 is an essential transcription factor for erythroid differentiation, known to be implicated in hematological conditions presenting with IE, including beta-thalassemia and congenital dyserythropoietic anemia. However, little is known about the role of GATA1 in the erythropoietic defects recently described in sickle cell anemia (SCA). In the present study, we performed a detailed characterization of the role of GATA1 and ineffective erythropoiesis in SCA using both *in-vitro* and *in-vivo* assay systems. We demonstrate a significant decrease in GATA1 protein levels during SCA erythropoiesis and a concomitant increase in oxidative stress. Furthermore, we found that an increase in the activity of the inflammatory caspase, caspase 1, was driving the decrease in GATA1 levels during SCA erythropoiesis and that, upon inhibition of caspase 1 activity, SCA erythropoiesis was rescued and GATA1 levels partially restored. Our study further elucidates the defect in erythropoiesis in SCA, and may therefore help in the development of novel approaches to normalise the bone marrow niche prior to stem cell transplantation, or facilitate the production of healthy stem cells for gene therapy.

Introduction

Sickle cell anemia (SCA) is a recessively inherited disease and one of the most common severe monogenic disorders worldwide(1) affecting more than 8 million people. SCA is due to a single mutation in the β-globin chain (β^S) of human hemoglobin resulting in HbS. This abnormal haemoglobin polymerizes in the deoxygenated state and causes the pathognomic red blood cell (RBC) sickling. Although every person with SCA has the same underlying genotype, being homozygous for the β-globin variant (HBB; c.20A>T,p.Glu7Val), it is a remarkably variable condition, with a wide range of clinical manifestations.

Ineffective erythropoiesis is known as the abnormal differentiation of erythroid progenitors accompanied by an expanded progenitor compartment, increased destruction of abnormal erythroblasts and a paucity in the production of mature erythroid cells. It is recognized as an important factor in many types of anemia, including beta-thalassemia (2, 3). However, it has not been systematically investigated in SCA. In a recent study, it was shown that erythroblasts from the bone marrow of sickle mice had increased reactive oxygen species (ROS) production and an increased level of apoptosis, both of which are characteristics of ineffective erythropoiesis (4). In another study using both *in-vivo* human derived erythroblasts and *in-vitro* erythroblasts produced from SCA patients, the extent of ineffective erythropoiesis in SCA was evaluated (5). By mimicking the hypoxic environment of the bone marrow niche, this work showed that hypoxia induces high levels of apoptosis during erythropoiesis in SCA, suggesting that disordered erythropoiesis is a feature of SCA(5). More recently, using the sickle Townes mouse model, impaired erythropoiesis was observed in the bone marrow, characterized by a remarkable decrease in erythroblast levels in bone marrow when compared to the relevant control(6).

GATA1, the founding member of the GATA factor family of transcription factors, is critical for the differentiation of the erythroid lineage. Together with orchestrating the expression of erythroid-specific genes, GATA1 controls the growth, differentiation, and survival of the erythroid lineage(7). GATA1 is known to be downregulated in hematological conditions presenting with abnormal erythropoiesis including beta-thalassemia and Diamond-Blackfan Anemia(8, 9). However, little is known about the role of GATA1 in the erythropoietic defects observed in SCA.

In the present study, we performed a detailed characterization of the role of GATA1 and ineffective erythropoiesis in SCA using both *in-vitro* and *in-vivo* assay systems. We documented in both systems a decrease in GATA1 protein levels during SCA erythropoiesis and a concomitant increase in oxidative stress levels. Mechanistically, we found that an

increase in the activity of the inflammatory caspase, caspase 1, was behind the decrease in GATA1 levels during SCA erythropoiesis. Notably, upon the inhibition of caspase 1 activity, SCA erythropoiesis was rescued and GATA1 levels partially restored.

Methods

Cell lines

Human Umbilical Cord Blood-Derived Erythroid Progenitor-2 (HUDEP-2) cell line was obtained from the Nakamura lab under an MTA agreement (10). The sickle HUDEP-2 (sHUDEP-2) cell line was obtained from the Tisdale lab under an MTA agreement (11).

Human biological samples

This study was conducted according to the declaration of Helsinki with approval from the Health Research Authority (HRA) and Health and Care Research Wales (HCRW) (Reference number: 21/WS/0117). Blood samples were obtained from sickle cell anemia (SS) patients and Healthy Donors (HD) after informed written consent at King's College Hospital (KCH, London, United Kingdom).

Mouse Model

Berkeley mice (The Jackson Laboratory, Stock# **003342**) were maintained in the King's College London Biological Service Unit (BSU), Guy's campus. Genotyping and breeding were performed as recommended by The Jackson Laboratory. Mice were housed and handled according to UK Home Office guidelines (Project Licence: P5741188). All animal experiments were approved by the Named Animal Care and Welfare Officer (NACWO). Adult male and female mice aged between 4 – 5 months were used in this study, and in each experiment equal number of male and female mice were used. Details of mice experiments are listed in the supplementary method section.

Laboratory Methods

HUDEP-2 and sHUDEP-2 cells were cultured as previously described(12). Peripheral blood mononuclear cells (PBMCs) were isolated from blood samples using after Percoll fractionationation and magnetic beads. CD34+ cells were cultured in an *in-vitro* two phase liquid culture system as previously described(5). Further information, including details of antibodies used, flow cytometry, measurement of reactive oxygen species, GATA1 staining,

the caspase assay, analysis of mouse spleen and bone marrow, imaging flow cytometry, and mass cytometry are given in the supplementary method section.

Statistical Analysis

Statistical analysis was performed using Graphpad Prism (version 9). Data was analyzed using the Mann-Whitney unpaired test.

Results

Delayed terminal erythroid differentiation in human SS erythroblasts

We first tested a human HUDEP-2-derived proerythroblast cell line in which the sickle mutation was introduced by gene editing in both β-globin alleles (hereafter referred to as SS HUDEP-2 cells) (11). We induced differentiation of both SS and wild type (WT) HUDEP-2 cells and monitored differentiation kinetics using flow cytometry and microscopy. At day 0 of differentiation, both WT and SS HUDEP-2 cells are at the proerythroblast stage, shown by Band3 and CD49d staining (Supp. Fig. 1A). Differentiation kinetics were similar between both WT and SS HUDEP-2 at days 2 and 4 (Supp.Fig. 1A,B,D). At day 6, however, a slight delay in differentiation was observed in the SS HUDEP-2 cell line, also evidenced by the significantly fewer orthochromatic erythroblasts (Supp. Fig.1A,C,E).

We next tested primary CD34+ cells isolated from the peripheral blood of healthy donors (HD) and patients with SCA (homozygous for the sickle mutation, SS) and cultured in a two-phase differentiation system(5). Differentiation kinetics were monitored during phase 2 of the culture (Supp. Fig.2). The percentage of GPA positive cells was evaluated as a reflection of the commitment of the CD34+ cells to the erythroid lineage. Significantly fewer GPA positive cells were observed in the SS compared to the HD cultures, indicating an alteration in the commitment of SS progenitors to the erythroid lineage (Supp. Fig. 3 A-B). We assessed the erythroid differentiation kinetics of the GPA positive cell population only, by profiling the CD49d and Band3 cell surface markers. In SS cultures, a striking delay in differentiation was observed compared to HD cultures, starting from day 2 of Phase 2 (Supp Fig. 4A-C). Most erythroblasts in the SS cultures were at the proerythroblast stage at day 4, while the HD cells were at the basophilic stage. At day 6 of differentiation, 52.9% (SD:12.5) of HD cells were at the polychromatic stage, compared to 15.0% (SD: 9.9) for the SS cells (Supp Fig. 4B-C). Likewise, by day 8, 41.8% (SD: 18.2) of HD cells had reached the orthochromatic stage, compared to only 4.8% (SD: 5.39) of SS cells (Supp Fig. 4B-C). Overall, we observed a marked delay in the differentiation of SS erythroblasts compared to

HD, when placed in similar culture conditions. Moreover, we did not see such a marked delay in the differentiation kinetics of the SS HUDEP-2 cells.

Increased oxidative stress in human SS erythroblasts

To assess oxidative stress in SS erythropoiesis, the levels of reactive oxygen species (ROS) were monitored during phase 2 of differentiation in the WT and SS HUDEP-2 cell lines. The mean fluorescence intensity (MFI) levels were measured and normalized according to the ROS levels in WT cells at day 2, 4, and 6 of differentiation. From this analysis, no differences in ROS levels were detected when comparing the WT and SS HUDEP-2 cell lines, during differentiation (Suppl. Fig. 5A- B).

Similar analysis was also performed in the HD and SS primary cultures, with ROS levels monitored at days 2, 4, 6 and 8 of phase 2 of differentiation. ROS levels were higher in the SS cultures compared to HD, starting from day 2 and up until day 8, which was the last time point of differentiation tested (Fig. 1A-B). Specifically, ROS MFI levels in SS cells were 15242 higher (SD: 8439) compared to 8040 (SD: 2862) in HD cells at day 2 of differentiation, further increasing in SS cells to 17149 on day 4 (SD: 8933), compared to 3594 (SD: 1591) in HD cells. ROS levels remained high through days 6 in SS cells (5836, SD: 2907) and 8 of differentiation (2106, SD: 621) when compared to HD cells (day 6: 2094, SD: 1637; day 8: 914, SD: 68) (Fig. 1A-B). Notably, increased ROS levels were apparent from early erythroid development, before significant amounts of sickle hemoglobin are present in the cells.

GATA1 levels are decreased in differentiating human SS erythroblasts

Many defects in erythropoiesis are characterized by aberrant GATA1 protein expression(13, 14, 15). Hence, GATA1 protein levels were assessed in the HD and SS primary cultures using classical flow cytometry, western blot analysis and cytometry by time of flight (CyTOF) technology (Suppl. Fig. 2). Using flow cytometry, MFI levels of GATA1 protein in GPA positive erythroblasts were measured and compared to GATA1 levels in HD erythroblasts (Fig. 2A-B). A significant decrease in GATA1 MFI levels was detected in the SS erythroblasts when compared to HD erythroblasts (Fig. 2A-B). Specifically, at day 2 the MFI of GATA1 in HD erythroblasts was at a mean of 4414 (SD:1066) compared to 1744 (SD: 838) in SS erythroblasts. At day 6 the MFI of GATA1 in HD was 4107 (SD:1288) while in SS erythroblasts GATA1 levels were significantly less (1681, SD: 981) (Fig. 2A-B). To confirm the low GATA1 levels, nuclear protein extracts were prepared from HD and SS

erythroblasts at days 6 and 8 of differentiation and GATA1 protein levels were measured by western immunoblotting analysis and normalized to β-actin levels (Fig. 2C-D). GATA1 levels were very low to undetectable in the cytoplasmic fraction we therefore focused our analysis on nuclear extracts of erythroblasts. A decrease in GATA1 was again observed in the SS nuclear extracts when compared to HD on both days, with a more significant decrease observed on day 8 of differentiation (Fig. 2C-D). Moreover, GATA1 levels were measured by CyTOF at D6, in stage matched erythroblasts, that were identified using the GPA and CD71 surface markers, HD and SS erythroblasts. From this it was evident that GPA+ CD71+ SS erythroblasts had lower levels of GATA1, indicated by a shift to the left in the cell population, when compared to GPA+ CD71+ HD erythroblasts (Fig. 2E-F). Taken together, this confirms that SS erythroblasts express less GATA1 protein when compared to HD erythroblasts. To evaluate whether the decrease in GATA1 is at the post-transcriptional level, we measure GATA1 mRNA at day 6. GATA1 mRNA levels were similar between HD and SS erythroblasts (Supp. Fig .6).

GATA1 protein levels were also assessed during differentiation of the SS and WT HUDEP-2 cell lines. In line with our observations of no difference in differentiation kinetics, we saw no significant difference by Western blot analysis in GATA1 protein levels in WT and SS HUDEP-2 cells throughout differentiation (Supp. Fig. 7A- B).

NRF2 and FOXOA3 levels are altered in SS erythroblasts

Nuclear factor, erythroid derived 2 (NRF2) and Forkhead box O3 (FOXO3a) are transcription factors that are known to be required for the regulation of cellular oxidative stress response genes(16, 17). Since we observed higher ROS levels in the SS cells during differentiation (Fig. 1), we investigated how this was reflected in the levels of NRF2 and FOXO3a proteins in the HD and SS erythroblasts at days 6 and 8 of differentiation. We found that, on both days, NRF2 and FOXO3a levels were significantly lower in the SS erythroblasts, as compared to HD (Fig. 2G-H). This is particularly evident on day 8 of differentiation, when very little NRF2 and FOXO3a proteins were detectable (Fig. 2G). FOXO3a levels were also assayed by CyTOF in the GPA+CD71+ erythroblasts from a HD and an SS patient. Again, we found FOXO3a levels to be significantly lower in GPA+CD71+ SS erythroblasts, compared to HD (Fig. 2E-F).

The bone marrow and spleen of SS Berkeley mice exhibit a disrupted architecture

SS Berkley mice have targeted deletions of the murine α and ß globins and carry transgenes containing the human α, β^S, γ^A and γ^G globin genes(18, 19). Thus, these mice exclusively express human sickle hemoglobin (20). We used Berkeley SS mice to investigate defects in erythropoiesis, with HbAS Berkeley mice used as a control (Supp. Fig. 8)(21).

As a validation for the model in our hands, hemoglobin levels were measured and found to be lower in the SS mice (mean: 6.6g/dL, SD: 0.92) as compared to the AS mice (mean: 11g/dL, SD: 0.95) (Supp. Fig. 9A). Animal weight was also lower in the SS mice (mean: 26.62g, SD: 6.92) compared to AS mice (mean: 36.86g, SD: 6.02) used in this study (Supp. Fig. 9B). Moreover, spleen weight, which is a well-known characteristic of this mouse model, was much higher in the SS mice (mean: 0.99g, SD: 0.18) as compared to the AS mice (mean: 0.1g, SD:0.02) (Supp. Fig. 9C).

As both the bone marrow and spleen are erythropoietic niches in mice, histological analysis by hematoxylin and eosin (HE) staining was performed on both tissues. Sections of bone marrow from the femur were analyzed and the SS mice showed noticeable clumping of hematopoietic cells and an increased number of erythroid precursors (Supp. Fig. 9D). The spleen of SS mice exhibited a disrupted architecture, with a complete loss of well-defined compartments of red and white pulp (Supp. Fig. 9E). Using Perl's staining, we also observed an increase of iron deposits in the SS mice (Supp. Fig. 9E). All the above observations are hallmarks of sickle cell pathology and are consistent with previous work on the pathology of the Berkeley SS mice(20, 21).

Delayed erythroid differentiation in the bone marrow and spleen of SS Berkeley mice

We next assessed the levels of Ter119, a specific marker for murine erythropoiesis, in cells isolated from both the bone marrow and the spleen of the SS and AS Berkeley mice, as a reflection of erythropoietic activity in these tissues. An increased percentage of Ter119+ cells was observed in the bone marrow (mean: 42.84%, SD:10.8) and spleen (mean:41.69%, SD: 18.16) of SS mice compared to the bone marrow (mean: 29.64%, SD:8.6) and spleen of AS (mean: 5.21%, SD:5.9) (Fig. 3A-B).

We next assessed the differentiation kinetics during erythropoiesis, by characterizing the levels of EryA (Basophilic Erythroblasts), EryB (Polychromatic Erythroblasts) and EryC (Orthochromatic erythroblasts), that were defined using Ter119 and CD71 staining in hematopoietic cells isolated from the bone marrow and spleen of SS and AS mice(22). The SS bone marrow cells had a significantly higher percentage of EryA (SS:50.01%, SD:1.27; AS:36.86%, SD: 5.88) and a significantly lower percentage of EryC (SS: 9.66%, SD: 1.5;

AS: 21.46%, SD: 3.7) (Fig. 3C; Supp Fig. 10A). The spleen isolates of SS mice exhibited a similar profile to that of the bone marrow cells, with a significantly lower percentage of Ery C (36.7%, SD:5.97), when compared to the EryC population in AS (85.16%, SD: 8.79) (Fig. 3D; Supp Fig. 10B). These findings demonstrate that there is a delay in erythroid differentiation similar to that seen in the *ex-vivo* analysis of CD34+ cells from sickle patients, described above.

Next, HSCs were isolated from the bone marrow of AS and SS mice and placed in an ex-vivo culture system for 4 days(23). Differentiation kinetics were monitored at days 2 and 4 of culture using Ter119 and CD71 staining, as described above. At day 2, the SS culture had higher EryA and lower EryB when compared to AS (Fig. 4A and C). Moreover, at day 4 the SS culture had higher EryB and lower EryC when compared to AS (Fig. 4B and D). Therefore, delayed differentiation was again observed in SS, in keeping with our findings above.

Increased oxidative stress in the bone marrow and spleen of SS Berkeley mice

ROS levels were measured in (i) red cells from peripheral blood, (ii) cells isolated from the bone marrow aspirates and (iii) spleen cells from AS and SS mice. We found that MFI levels were higher in the SS red cells, as compared to AS (Fig. 3E-F). ROS MFI levels were also significantly higher in the bone marrow and spleen cells isolated from the SS mice, as compared to the AS (Fig. 3G). This is, again, in accordance with the increased oxidative stress seen in the human sickle erythroblasts (Fig. 1).

Decreased GATA1 levels in erythroblasts of SS Berkeley mice

GATA1 protein levels were assessed in erythroblasts isolated from the bone marrow and spleen tissues of the AS and SS mice. Isolated cells were stained using Ter119 antibody and sorted using the gating strategy shown in Supp. Fig. 11. Nuclear extracts were isolated from Ter119+ sorted erythroblasts and GATA1 protein levels were assessed by Western blotting. GATA1 levels were decreased in Ter119+ erythroblasts from both SS bone marrow and spleen, as compared to AS cells (Fig. 5A-D).

GATA1 protein was also assessed by measuring GATA1 MFI levels in the Ter119+ population by flow cytometry. GATA1 MFI was significantly decreased in SS bone marrow erythroblasts as compared to AS (Fig. 5E). A similar pattern was observed in spleen Ter119+ erythroblasts (Fig. 5E). To further validate these findings, imaging flow cytometry was used to assess GATA1 levels in SS stage matched erythroblasts. Using a novel analysis pipeline

(Supp. Fig. 12), bone marrow and spleen cells were double stained for Ter119 and GATA1. As Ter119+ cells include erythroblasts, reticulocytes, or mature red cells, we used the IDEAS software to set up an analytical pipeline based on the perimeter and H-variance features, to specifically gate for the erythroblast population (Supp. Fig. 12). We then discriminated between two populations of GATA1 erythroblasts, the GATA1 Low Erythroblasts, expressing less GATA1 in the nucleus and the GATA1 High Erythroblasts, expressing more GATA1 in the nucleus (Fig. 6A-D). Using this approach, we found that there were significantly fewer GATA1 High Erythroblasts in the bone marrow and spleen of SS mice, as compared to AS mice (Fig. 6C).

Increased caspase 1 activity in the bone marrow and spleen of SS Berkeley mouse

Recently, manipulation of inflammasome components, specifically caspase 1, was shown to alter the differentiation of hematopoietic stem and progenitor cells (24). It was also reported that GATA1 was susceptible to specific cleavage by caspase 1 in the erythroblastic K562 cell line(25). As we have shown that inflammation is a characteristic of SS erythropoiesis, we investigated caspase 1 activity in the different erythroblast populations (EryA, EryB and EryC) in the bone marrow and spleen of SS and AS mice. In the bone marrow, caspase-1 activity was higher in all SS erythroblast populations compared to AS, with EryBs (Polychromatic Erythroblasts) showing the highest activity (Fig. 7A). In the spleen, a similar pattern was observed, with higher levels of caspase 1 activity in the SS erythroblasts as compared to AS (Fig. 7B). Note that the EryA population was not studied in the spleen, due to a very low percentage of EryA in spleen of AS mice. Lin negative cells were isolated from the bone marrow of AS and SS mice and placed in an ex-vivo culture system for 4 days and caspase 1 activity was measured in the Ter119+ erythroblasts at day 4 of differentiation. SS cultures had higher levels of caspase 1 activity, reflected by higher FLICA levels, an assay that labels active caspase 1, when compared to the AS cultures (Fig.7C).

Inhibition of Caspase 1 rescues human SS erythropoiesis

As our findings show that SS erythropoiesis is characterized by increased activity of caspase 1 and decreased GATA1 protein expression, we inhibited caspase 1 activity in SS cultures using the irreversible inhibitor Ac-YVAD-cmk(26). Upon treatment with Ac-YVAD-cmk (50μM), the differentiation kinetics of the SS culture were restored compared to the untreated culture, reaching levels closer to those of HD differentiation seen in Supplementary Figure 4 (Fig. 8A-B). GATA1 MFI levels were also assessed. An increase in GATA1 MFI levels was

observed at both D6 and D8 of differentiation in the Ac-YVAD-cmk treated cultures (Fig. 8C-D), in line with the rescued differentiation observed in the treated cultures. Upon treatment with Ac-YVAD-cmk, levels of GATA1 in SS erythroblasts became more comparable to those of HD erythroblasts (Supp. Fig. 13A). Nevertheless, ROS levels were not restored (Supp. Fig. 13B) this could be due to several reasons, (i) even though caspase 1 inhibition restors GATA1 levels, GATA1 might not be not solely responsible for oxidative stress regulation in erythropoiesis and thus other factors might be implicated; (ii) caspase 1 inhibition doesn't restore GATA1 to high enough levels to completely restore ROS levels.

Discussion

Defects in SCA erythropoiesis have been previously reported in the literature(4, 5, 6, 27). In this study we show that SCA erythropoiesis is characterized by a delayed differentiation both in our *in-vitro* model of primary cells and our *in-vivo* sickle mouse model. The latter is in line with the recent work of Han et al., showing that in the sickle Townes mouse the percentage of more differentiated erythroblasts was significantly less than in controls(6). However, we did not replicate these findings using the SS HUDEP-2 cell line, a cell line established by generating the sickle mutation in an immortalized human erythroid cell line (HUDEP-2)(11). This important finding suggests that the early abnormalities seen in erythropoiesis in SCA are a result of exposure to an abnormal bone marrow niche, rather than the sickle mutation itself. This may suggest that the effects of inflammation on erythropoietic progenitors persist even after these have been removed from the inflammatory environment, or possibly that the bone marrow niche selectively releases the more damaged stem cells into the circulation. The increased activity of the inflammasome-associated caspase 1 in the bone marrow and spleen of the SS mice and the partial rescue of erythropoiesis and of GATA1 protein levels on pharmacological inhibition of caspase 1, suggest that the abnormal erythropoiesis in SCA is, at least in part, caused by inflammation(28).

Our study also shows that oxidative stress levels are elevated during SCA erythropoiesis, and this likely also contributes to the abnormal erythropoiesis. Oxidative stress in circulating RBCs is known to be increased in SCA(29, 30). We found that oxidative stress levels are also elevated in SCA erythroblasts, starting at the proerythroblast stage. Moreover, using the sickle mouse model, increased oxidative stress is observed in both the bone marrow and spleen cells. In line with the increased oxidative stress observed in SCA erythropoiesis, we show that the protein levels of NRF2 and FOXO3a, key transcriptional regulators of the oxidative stress response genes, are markedly reduced in the nuclei of human SS

erythroblasts. NRF2 is a master regulator of the antioxidant cell defense system. Activation of NRF2 by the ablation of its negative regulator Keap1 (Kelch-like ECH-associated protein 1), has been shown to significantly improve symptoms in a sickle mouse model and to reduce organ damage(31). Moreover, FOXO3a was identified as having an essential role regulating the oxidative stress response during erythropoiesis(17). Expression, nuclear localization, and transcriptional activity of FOXO3a are increased during physiological erythropoiesis(17, 32). Thus, the decrease in the nuclear protein levels of both FOXO3a and NRF2 we observe in SS erythroblasts, could contribute to the ineffective erythropoiesis observed in SCA. Note that, it is possible that other factors such as that KLF1, TAL1 and GATA2 could also be affected and contribute to the abnormal erythropoiesis in SCA.

Our study also shows that erythropoiesis is abnormal in SCA and that acquired GATA1 deficiency plays a major role in this. Both our *in vitro* and *in vivo* models show a significant decrease in GATA1 levels in SCA erythroblasts, when compared to the appropriate control. This decrease in GATA1 was shown by a number of assays and cannot be explained by differences in differentiation stage between SS and HD erythroblasts alone. Instead, we suggest that reduced GATA1 levels may be the cause of the delay in differentiation observed in SCA. Whether decreased GATA1 levels in SCA erythroblasts are responsible for the decrease in NRF2 and FOXO3a levels, is yet to be investigated. Previously, HSP70, a chaperone protein known to protect GATA1 from cleavage by caspase 3 during erythropoiesis, was investigated in SCA erythropoiesis and shown to interact with HbS polymers under hypoxia. Moreover, HSP70 sequestration in the cytoplasm of SCA erythroblasts was also observed(5). This is similar to observations made in the ineffective erythropoiesis of beta-thalassemia. In our study, we identify a novel mechanism responsible for the decrease of GATA1 levels during SCA erythropoiesis, via the activation of caspase 1. Our data show an increase in the activity of caspase 1, an inflammatory caspase, in SCA erythroblasts. Moreover, inhibition of caspase 1 activity partially restored GATA1 levels during SCA erythropoiesis. Therefore, we propose that a decrease in GATA1 levels during SCA erythropoiesis is due to both caspase 3 activation, leading to HSP70 sequestration in the cytoplasm, and caspase 1 activation through the inflammasome. Importantly, we show that the pharmacological inhibition of caspase 1 alleviates ineffective erythropoiesis, thus making it a druggable target in treating SCA. Note that caspase 1 activation, via the formation of inflammasome complex, is known to initiate a pro-inflammatory response through the cleavage of two inflammatory cytokines IL-1β and IL-18, both of which are known to be

increased in the plasma of SCA patients(33, 34, 35) . Therefore the inhibition of caspase 1 could be restoring erythropoiesis by both increasing levels of GATA1 and decreasing the pro-inflammatory response. Further analyses are required to investigate in depth the role of caspase 1 in inducing inflammation during SCA erythropoiesis.

Overall, our paper contributes to the emerging evidence that ineffective erythropoiesis occurs in SCA, with significant numbers of erythroid precursors failing to mature into circulating red cells(36). This involves several components: late stage erythropoiesis is impaired by the polymerisation of deoxygenated HbS, which damages the cells, prevents maturation and generates oxidative stress and inflammation[7]; this is further amplified by circulating sickle cells infarcting areas of bone marrow and causing sterile inflammation from haemolysis and the release of free haemoglobin. This oxidative stress and inflammation further impair erythropoiesis by activating caspase 1 and causing acquired GATA1 deficiency. Overall, this generates a hostile bone marrow niche and results in the production of abnormal haematopoietic stem cells which fail to mature properly. This is particularly relevant in the context of hematopoietic stem cell based therapies, including transplantation, gene addition and gene editing, and the need to work with healthy stem cells and a receptive bone marrow niche to optimise outcomes. This study helps to define the precise nature of the defect in sickle erythropoiesis, and may help develop novel approaches to normalise the bone marrow niche prior to stem cell transplantation or facilitate the production of healthy stem cells for gene therapy.

References

1. Weatherall D, Hofman K, Rodgers G, Ruffin J, Hrynkow S. A case for developing North-South partnerships for research in sickle cell disease. Blood. 2005;105(3):921-923.
2. Arlet JB, Ribeil JA, Guillem F, et al. HSP70 sequestration by free alpha-globin promotes ineffective erythropoiesis in beta-thalassaemia. Nature. 2014;514(7521):242-246.
3. Ribeil JA, Arlet JB, Dussiot M, Moura IC, Courtois G, Hermine O. Ineffective erythropoiesis in beta -thalassemia. ScientificWorldJournal. 2013;2013:394295.
4. Park SY, Matte A, Jung Y, et al. Pathologic angiogenesis in the bone marrow of humanized sickle cell mice is reversed by blood transfusion. Blood. 2020;135(23):2071-2084.
5. El Hoss S, Cochet S, Godard A, et al. Fetal hemoglobin rescues ineffective erythropoiesis in sickle cell disease. Haematologica. 2021;106(10):2707-2719.
6. Han Y, Gao C, Liu Y, et al. Hemolysis-driven IFNalpha production impairs erythropoiesis by negatively regulating EPO signaling in sickle cell disease. Blood. 2023;143(11):1018-1031.
7. Gutierrez L, Caballero N, Fernandez-Calleja L, Karkoulia E, Strouboulis J. Regulation of GATA1 levels in erythropoiesis. IUBMB Life. 2020;72(1):89-105.
8. Frisan E, Vandekerckhove J, de Thonel A, et al. Defective nuclear localization of Hsp70 is associated with dyserythropoiesis and GATA-1 cleavage in myelodysplastic syndromes. Blood. 2012;119(6):1532-1542.
9. Iskander D, Wang G, Heuston EF, et al. Single-cell profiling of human bone marrow progenitors reveals mechanisms of failing erythropoiesis in Diamond-Blackfan anemia. Sci Transl Med. 2021;13(610):eabf0113.
10. Kurita R, Suda N, Sudo K, et al. Establishment of immortalized human erythroid progenitor cell lines able to produce enucleated red blood cells. PLoS One. 2013;8(3):e59890.
11. Demirci S, Gudmundsdottir B, Li Q, et al. betaT87Q-Globin Gene Therapy Reduces Sickle Hemoglobin Production, Allowing for Ex Vivo Anti-sickling Activity in Human Erythroid Cells. Mol Ther Methods Clin Dev. 2020;17:912-921.
12. Hawksworth J, Satchwell TJ, Meinders M, et al. Enhancement of red blood cell transfusion compatibility using CRISPR-mediated erythroblast gene editing. EMBO Mol Med. 2018;10(6):e8454.
13. Ludwig LS, Gazda HT, Eng JC, et al. Altered translation of GATA1 in Diamond-Blackfan anemia. Nat Med. 2014;20(7):748-753.
14. Gilles L, Arslan AD, Marinaccio C, et al. Downregulation of GATA1 drives impaired hematopoiesis in primary myelofibrosis. J Clin Invest. 2017;127(4):1316-1320.
15. Arlet JB, Ribeil JA, Guillem F, et al. HSP70 sequestration by free alpha-globin promotes ineffective erythropoiesis in beta-thalassaemia. Nature. 2014;514(7521):242-246.
16. Zhu X, Xi C, Thomas B, Pace BS. Loss of NRF2 function exacerbates the pathophysiology of sickle cell disease in a transgenic mouse model. Blood. 2018;131(5):558-562.
17. Marinkovic D, Zhang X, Yalcin S, et al. Foxo3 is required for the regulation of oxidative stress in erythropoiesis. J Clin Invest. 2007;117(8):2133-2144.
18. Paszty C, Brion CM, Manci E, et al. Transgenic knockout mice with exclusively human sickle hemoglobin and sickle cell disease. Science. 1997;278(5339):876-878.
19. Woodard KJ, Doerfler PA, Mayberry KD, et al. Limitations of mouse models for sickle cell disease conferred by their human globin transgene configurations. Dis Model Mech. 2022;15(6):dmm049463.

20. Manci EA, Hillery CA, Bodian CA, Zhang ZG, Lutty GA, Coller BS. Pathology of Berkeley sickle cell mice: similarities and differences with human sickle cell disease. Blood. 2006;107(4):1651-1658.
21. Szczepanek SM, McNamara JT, Secor ER, Jr., et al. Splenic morphological changes are accompanied by altered baseline immunity in a mouse model of sickle-cell disease. Am J Pathol. 2012;181(5):1725-1734.
22. Shim YA, Campbell T, Weliwitigoda A, Dosanjh M, Johnson P. Regulation of CD71(+)TER119(+) erythroid progenitor cells by CD45. Exp Hematol. 2020;86:53-66.e1.
23. Shuga J, Zhang J, Samson LD, Lodish HF, Griffith LG. In vitro erythropoiesis from bone marrow-derived progenitors provides a physiological assay for toxic and mutagenic compounds. Proc Natl Acad Sci U S A. 2007;104(21):8737-8742.
24. Rodriguez-Ruiz L, Lozano-Gil JM, Naranjo-Sanchez E, et al. ZAKalpha/P38 kinase signaling pathway regulates hematopoiesis by activating the NLRP1 inflammasome. EMBO Mol Med. 2023;15(10):e18142.
25. Tyrkalska SD, Perez-Oliva AB, Rodriguez-Ruiz L, et al. Inflammasome Regulates Hematopoiesis through Cleavage of the Master Erythroid Transcription Factor GATA1. Immunity. 2019;51(1):50-63.e5.
26. Tyrkalska SD, Candel S, Angosto D, et al. Neutrophils mediate Salmonella Typhimurium clearance through the GBP4 inflammasome-dependent production of prostaglandins. Nat Commun. 2016;7:12077.
27. Wu CJ, Krishnamurti L, Kutok JL, et al. Evidence for ineffective erythropoiesis in severe sickle cell disease. Blood. 2005;106(10):3639-3645.
28. Leonard A, Bonifacino A, Dominical VM, et al. Bone marrow characterization in sickle cell disease: inflammation and stress erythropoiesis lead to suboptimal CD34 recovery. Br J Haematol. 2019;186(2):286-299.
29. Quezado ZMN, Kamimura S, Smith M, et al. Mitapivat increases ATP and decreases oxidative stress and erythrocyte mitochondria retention in a SCD mouse model. Blood Cells Mol Dis. 2022;95:102660.
30. Lizarralde-Iragorri MA, Lefevre SD, Cochet S, et al. Oxidative stress activates red cell adhesion to laminin in sickle cell disease. Haematologica. 2021;106(9):2478-2488.
31. Keleku-Lukwete N, Suzuki M, Otsuki A, et al. Amelioration of inflammation and tissue damage in sickle cell model mice by Nrf2 activation. Proc Natl Acad Sci U S A. 2015;112(39):12169-12174.
32. Bakker WJ, Blazquez-Domingo M, Kolbus A, et al. FoxO3a regulates erythroid differentiation and induces BTG1, an activator of protein arginine methyl transferase 1. J Cell Biol. 2004;164(2):175-184.
33. Huang Y, Xu W, Zhou R. NLRP3 inflammasome activation and cell death. Cell Mol Immunol. 2021;18(9):2114-2127.
34. Gupta A, Fei YD, Kim TY, et al. IL-18 mediates sickle cell cardiomyopathy and ventricular arrhythmias. Blood. 2021;137(9):1208-1218.
35. Asare K, Gee BE, Stiles JK, et al. Plasma interleukin-1beta concentration is associated with stroke in sickle cell disease. Cytokine. 2010;49(1):39-44.
36. Brewin J, El Hoss S, Strouboulis J, Rees D. A novel index to evaluate ineffective erythropoiesis in hematological diseases offers insights into sickle cell disease. Haematologica. 2021;107(1):338-341.

Figures Legend

Figure 1: **Reactive oxygen species levels during erythroid differentiation in healthy donor (HD) and Sickle Cell Disease -SS genotype.** (A) A histogram showing the levels of reactive oxygen species (ROS) in HD (red) and SS (blue) cell at day 2, day 4, day 6 and day 8 of differentiation. (B) A line graph representing the mean fluorescence intensity (MFI) of ROS staining in HD and SS cells at day 2, day 4, day 6 and day 8 of differentiation (n=4), (mean ± standard deviation). *p<0.05, Mann-Whitney test.

Figure 2: **GATA1 protein levels in differentiating healthy donor (HD) and Sickle Cell Disease -SS genotype primary cells.** (A) A histogram showing the analysis by flow cytometry of GPA+ cells, assaying for GATA1 protein on days 2 and 6 of differentiation of HD (red) and SS (blue) cells. (B) Bar graph representing the mean fluorescence intensity (MFI) of GATA1 in the GPA+ population at day 2 and 6 of HD (red) and SS (blue) cell differentiation. (n=4). (mean ± standard deviation). (C) Western blot images of GATA1 (upper panel) and Actin (lower panel) proteins in nuclear extracts of HD and SS cells at days 6 and 8 of differentiation. (D) Bar graph representing the relative quantification by Western blotting of GATA1 protein levels in the nuclear extracts of HD and SS cells at days 6 and 8. Protein loading per lane for quantification was adjusted relative to Actin protein levels (n=4), (mean ± standard deviation). Histogram and density plot representations of GPA+ CD71+ cells showing the levels of protein expression of FOXO3a and GATA1 in (E) HD-010 and (F) SS-010. (G) Western blot analysis of NRF2 (upper panel), FOXO3a (middle pane) and Actin (lower panel) in nuclear extracts of differentiating HD and SS cells at days 6 and 8 of differentiation. (H) Bar graph showing the quantification of FOXO3a (left) and NRF2 (right) protein levels in nuclear extracts from HD and SS cells at days 6 and 8 of differentiation, relative to Actin protein levels (n=4) (mean ± standard deviation). *p<0.05, Mann-Whitney test.

Figure 3: **Erythropoiesis and oxidative stress in the AS and SS Berkeley mice.** (A) Histogram representing Ter119 expression in the bone marrow (left) and spleen (right) cells of one AS (green) and one SS (blue) mouse. (B) Bar graph representing the percentage of Ter119+ cells in the bone marrow and the spleen of AS (n=5) and SS (n=8) mice, (mean ± standard deviation). (C) A bar graph representing the percentage of Ery A, B and C cells in the bone marrow of AS and SS mice (n=7). (D) Bar graph representing the percentage of Ery

A, B and C cells in the spleen of AS and SS mice (n=7). (E) Histogram representing the levels of ROS in the peripheral blood of one AS (green) and one SS (blue) mouse. (F) Bar graph showing ROS mean fluorescence intensity (MFI) in the peripheral blood of AS (n=9) and SS (n=4) mice. (G) A bar graph representing ROS MFI in the bone marrow and spleen of AS and SS mice (n=5). (mean ± standard deviation). *p<0.05, **p<0.01, ***p<0.001 Mann-Whitney test.

Figure 4: **Ex-vivo erythroid differentiation of Lin negative cells from the bone marrow of AS and SS Berkeley mice.** A density plot representing the distribution of Ery A (basophilic), Ery B (polychromatic) and Ery C (orthochromatic) cells arising from ex vivo differentiated HSCs isolated from the bone marrow of one AS and one SS mouse, on (A) day 2 and (B) day 4 of culture. The plot represents CD71+ (y-axis) and FSC-H (x-axis). (C) Bar graph representing the percentage of Ery A and B on day 2 of ex-vivo differentiated bone marrow HSCs from AS and SS mice (n=2). (D) Bar graph representing the percentage of Ery B and C cells at day 4 of ex-vivo differentiated bone marrow HSCs from AS and SS mice (n=2), (mean ± standard deviation).

Figure 5: **GATA1 protein levels in bone marrow and spleen cells of SS and AS Berkeley mice.** (A) Western blot images of GATA1 (upper panel) and Actin (lower panel) proteins in nuclear extracts from Ter119+ cells, isolated from AS and SS bone marrow aspirates. (B) As in (A) using nuclear extracts from Ter119+ cells isolated from AS and SS spleens. (C) Bar graph representing quantification of GATA1 protein levels in the nuclear extracts of Ter119+ cells isolated from AS and SS bone marrow aspirates, relative to Actin levels (n=2). (D) Bar graph representing quantification of GATA1 protein levels in the nuclear extracts of Ter119+ cells isolated from AS and SS spleens, relative to Actin levels (n=4). (E) Bar graph representing the mean fluorescence intensity (MFI) of GATA1 in the Ter119+ population of the bone marrow (n=4) and spleen (n=4) of AS and SS mice (mean ± standard deviation).

Figure 6: **GATA1 protein levels in bone marrow and spleen cells of SS and AS Berkeley mice.** (A) Imaging flow cytometry (IFC) analysis graph representing the Max Pixel_MC_Ch02 GATA1 FITC on the x-axis and the Raw Max Pixel_MC_Ch02 GATA1 FITC on the y-axis. This analysis enables the discrimination between stage matched GATA1 Low Erythroblasts and GATA1 High Erythroblasts, within the Ter119+ Erythroblast cell population. (B) Histogram representing the distribution of GATA1 staining in the GATA1

Low Erythroblasts (light blue) and GATA1 High Erythroblasts (dark blue). (C) Bar graph representing the percentage of GATA1 High Erythroblasts in the bone marrow (n=4) and spleen (n=3) of AS and SS mice (mean ± standard deviation). (D) Representative images of a GATA1 Low Erythroblast (upper panel) and a GATA1 High Erythroblast (lower panel); images show Bright field, Ter119 (red), GATA1 (green) and the merged image. *$p<0.05$ Mann-Whitney test.

Figure 7: **Caspase 1 activity.** Bar graph representing the percentage of FLICA positive (Caspase 1 active) cells in (A) the bone marrow and (B) spleen of AS and SS mice. The percentage of FLICA positive cells is quantified in the EryA (bone marrow), EryB (bone marrow and spleen) and EryC (bone marrow and spleen) subpopulations (n=7). (C) Left panel: Histogram showing FLICA levels in Ter119+ erythroblasts on day 2 of *ex-vivo* differentiated Lin- cells from the bone marrow of one AS and one SS mouse; Right Panel: Bar graph representing the % FLICA positive Ter119+ cells on day 2 of *ex-vivo* differentiated Lin- cells from the bone marrow of one AS and one SS mouse. (n=2), (mean ± standard deviation).

Figure 8: **Inhibition of caspase 1 activity.** (A) A contour plot of GPA+ cells from phase 2 of differentiation of SS untreated (dark blue) and SS treated with Ac-YVAD-cmk (50µM) (light blue) CD34+ samples, showing the distribution of cell populations with respect to the expression of Band-3 FITC (x-axis) and CD49d-APC (y-axis). Data are represented for day 6 and day 8 of phase 2 of differentiation. Pro: Proerythroblast, EB: Early Basophilic, LB: Late Basophilic, Poly: Polychromatic, Ortho: Orthochromatic erythroblasts. (B) Images of SS untreated and Ac-YVAD-cmk treated cells at day 8 of culture stained with MGG. (C) A histogram showing the analysis by flow cytometry of GPA+ cells, assaying for GATA1 protein on days 6 and 8 of differentiation of SS untreated (dark blue) and SS Ac-YVAD-cmk treated (light blue) cells. (D) Bar graph representing the fold change in mean fluorescence intensity (MFI) of GATA1 in the GPA+ population at day 6 and 8 of SS untreated (dark blue) and SS Ac-YVAD-cmk treated (light blue) cells during differentiation. (n=3). (mean ± standard deviation). **$p<0.01$ Mann-Whitney

Figure 1

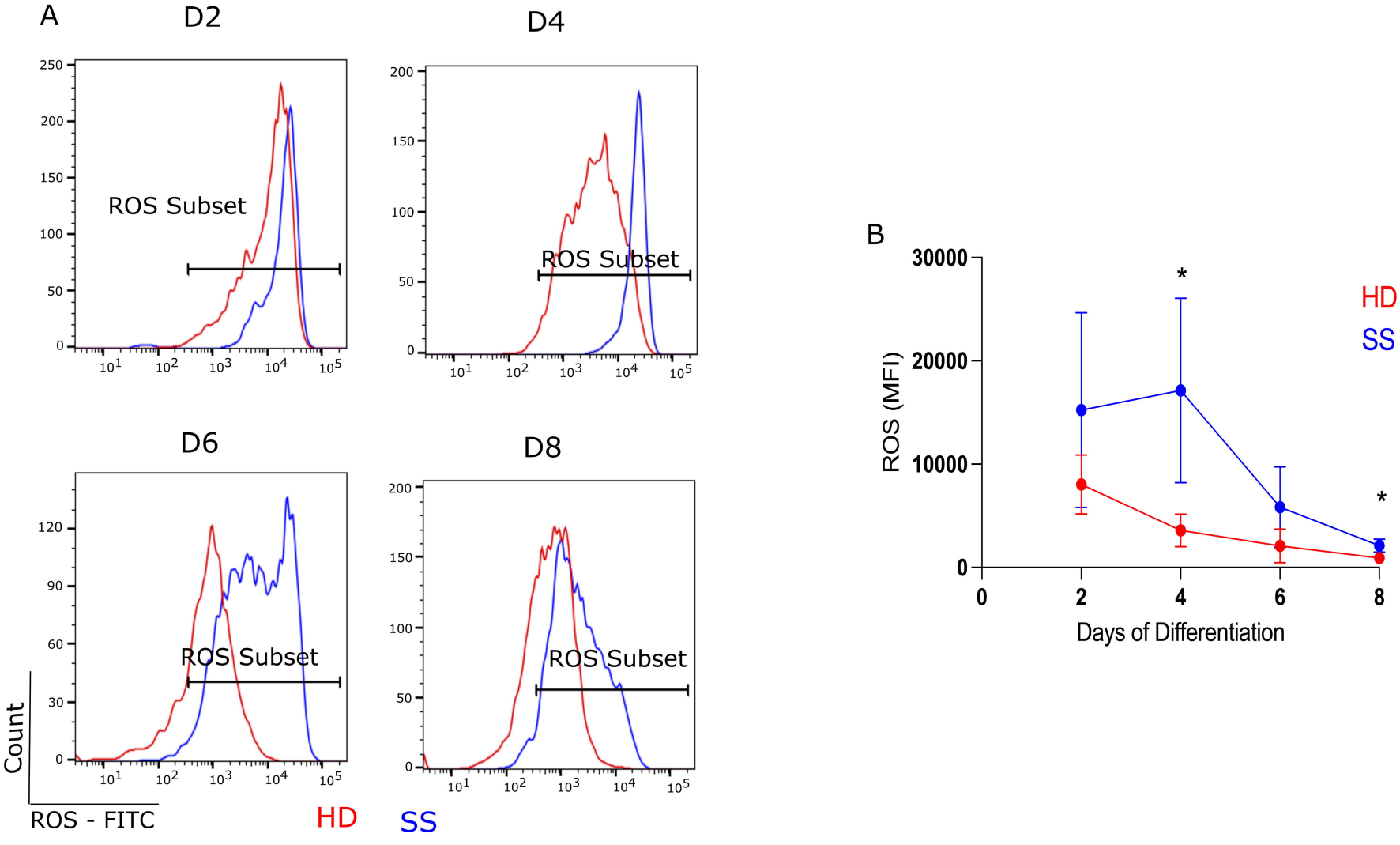
A
D2
D4
D6
D8
ROS Subset
Count
ROS - FITC
HD
SS
B
ROS (MFI)
Days of Differentiation
HD
SS
*
*

Figure 2

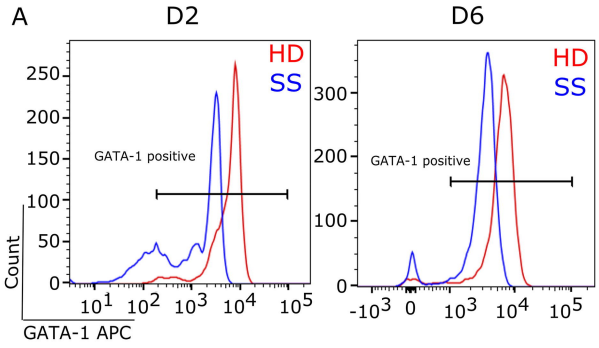
A
D2
D6
HD
SS
GATA-1 positive
Count
GATA-1 APC

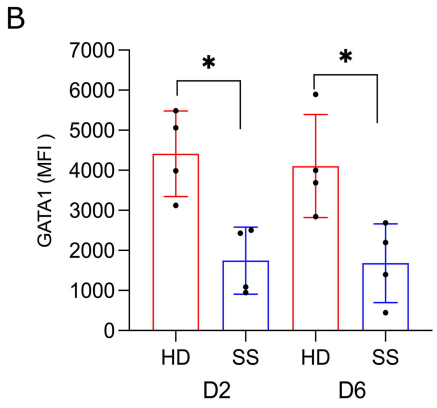
B
GATA1 (MFI)
HD
SS
D2
D6

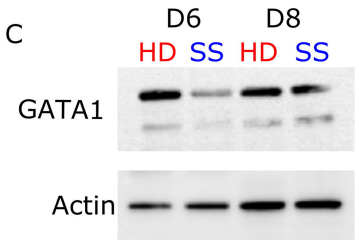
C
D6
D8
HD SS HD SS
GATA1
Actin

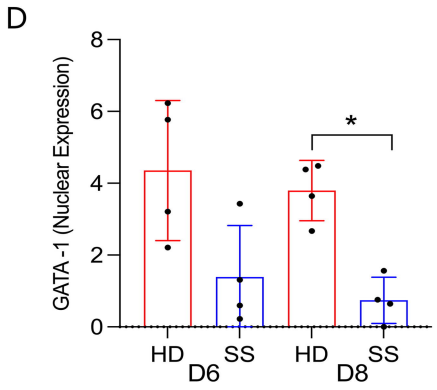
D
GATA-1 (Nuclear Expression)
HD
SS
D6
D8

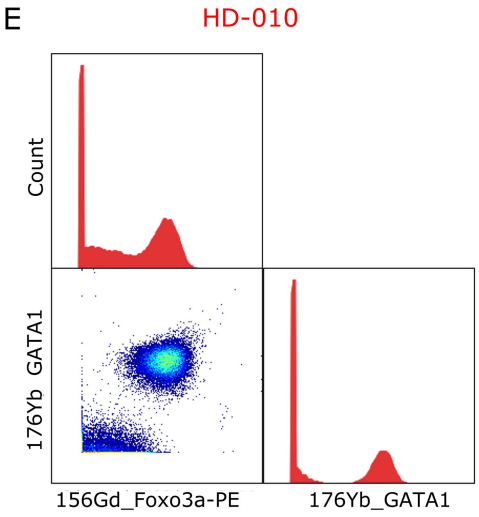
E
HD-010
Count
176Yb GATA1
156Gd_Foxo3a-PE
176Yb_GATA1

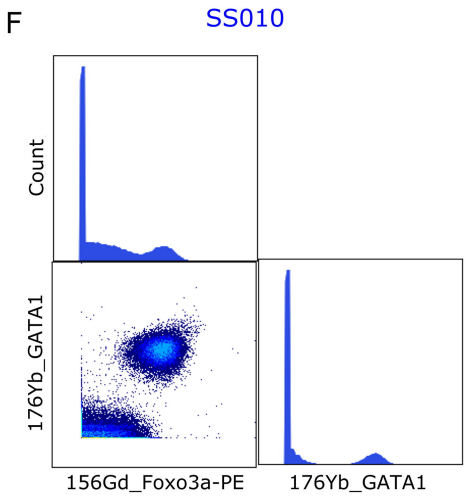
F
SS010
Count
176Yb_GATA1
156Gd_Foxo3a-PE
176Yb_GATA1

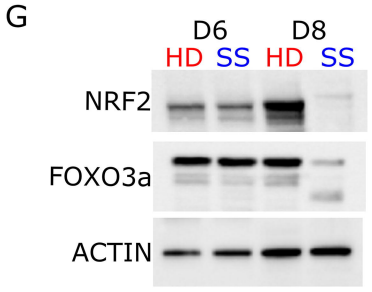
G
D6
D8
HD SS HD SS
NRF2
FOXO3a
ACTIN

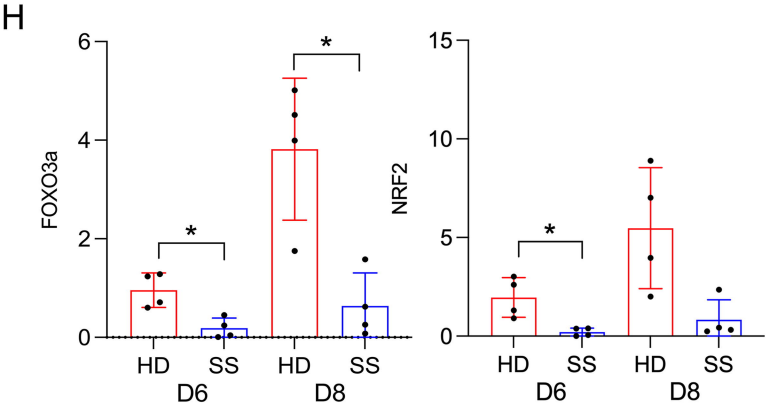
H
FOXO3a
NRF2
HD
SS
D6
D8

Figure 3

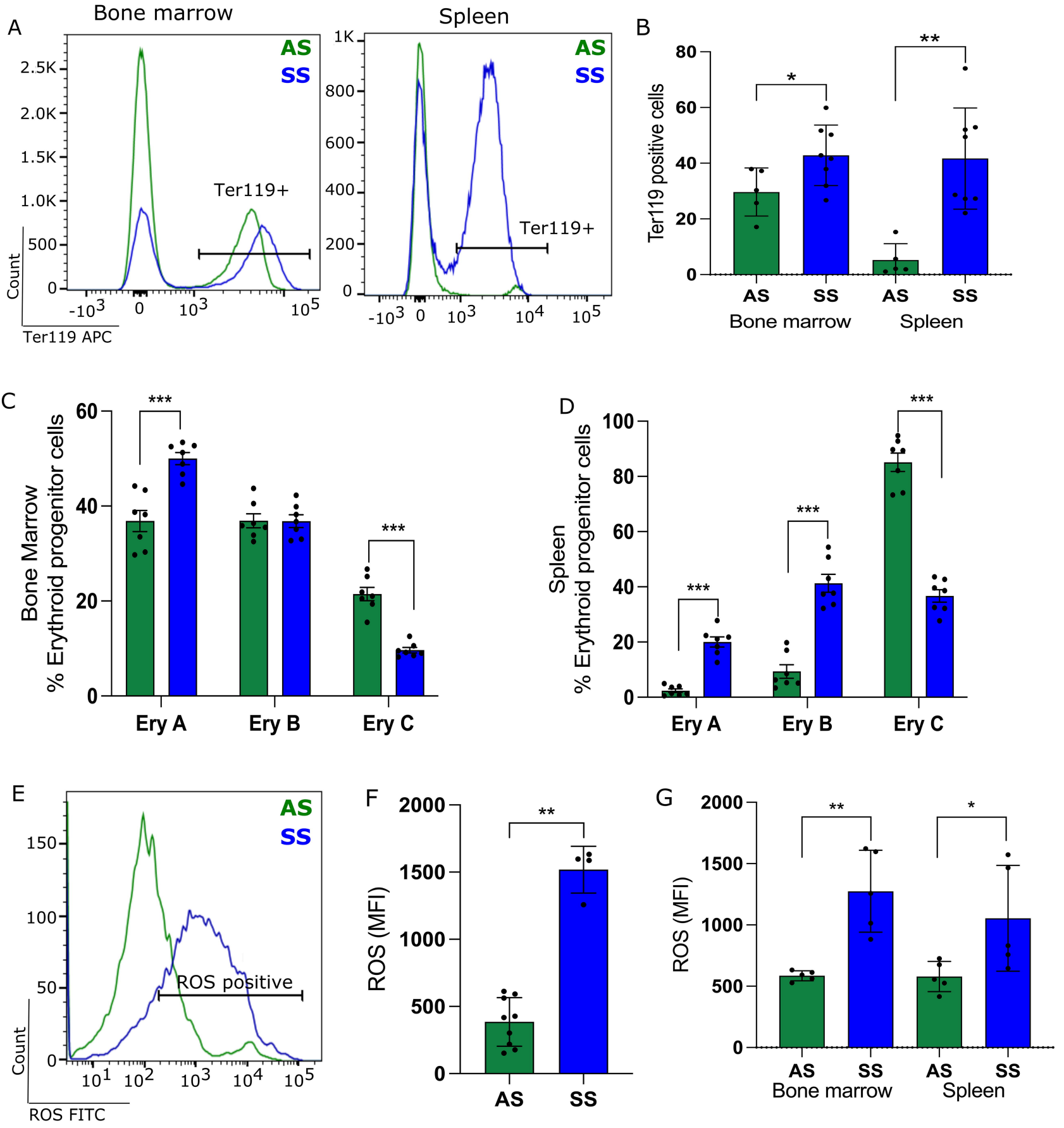
A
Bone marrow
Spleen
AS
SS
Ter119+
Count
Ter119 APC
B
Ter119 positive cells
Bone marrow
Spleen
C
Bone Marrow
% Erythroid progenitor cells
Ery A
Ery B
Ery C
D
Spleen
% Erythroid progenitor cells
E
ROS positive
ROS FITC
F
ROS (MFI)
G
ROS (MFI)

Figure 4

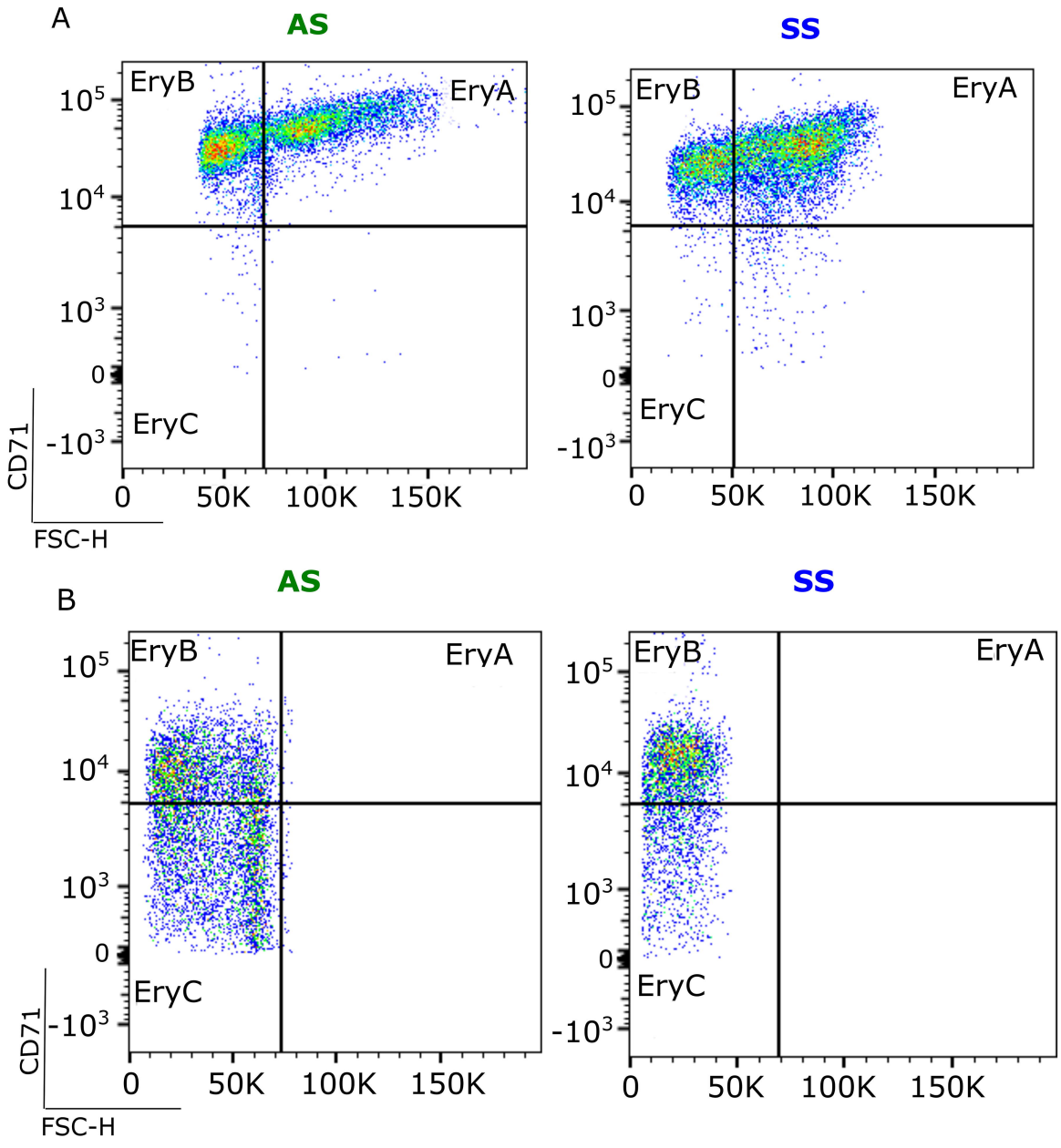
A
AS
SS
EryB
EryA
EryC
CD71
FSC-H
0
50K
100K
150K
B
C
D2
D4
%Erythroblasts
AS
SS
EryA
EryB
EryC

Figure 5

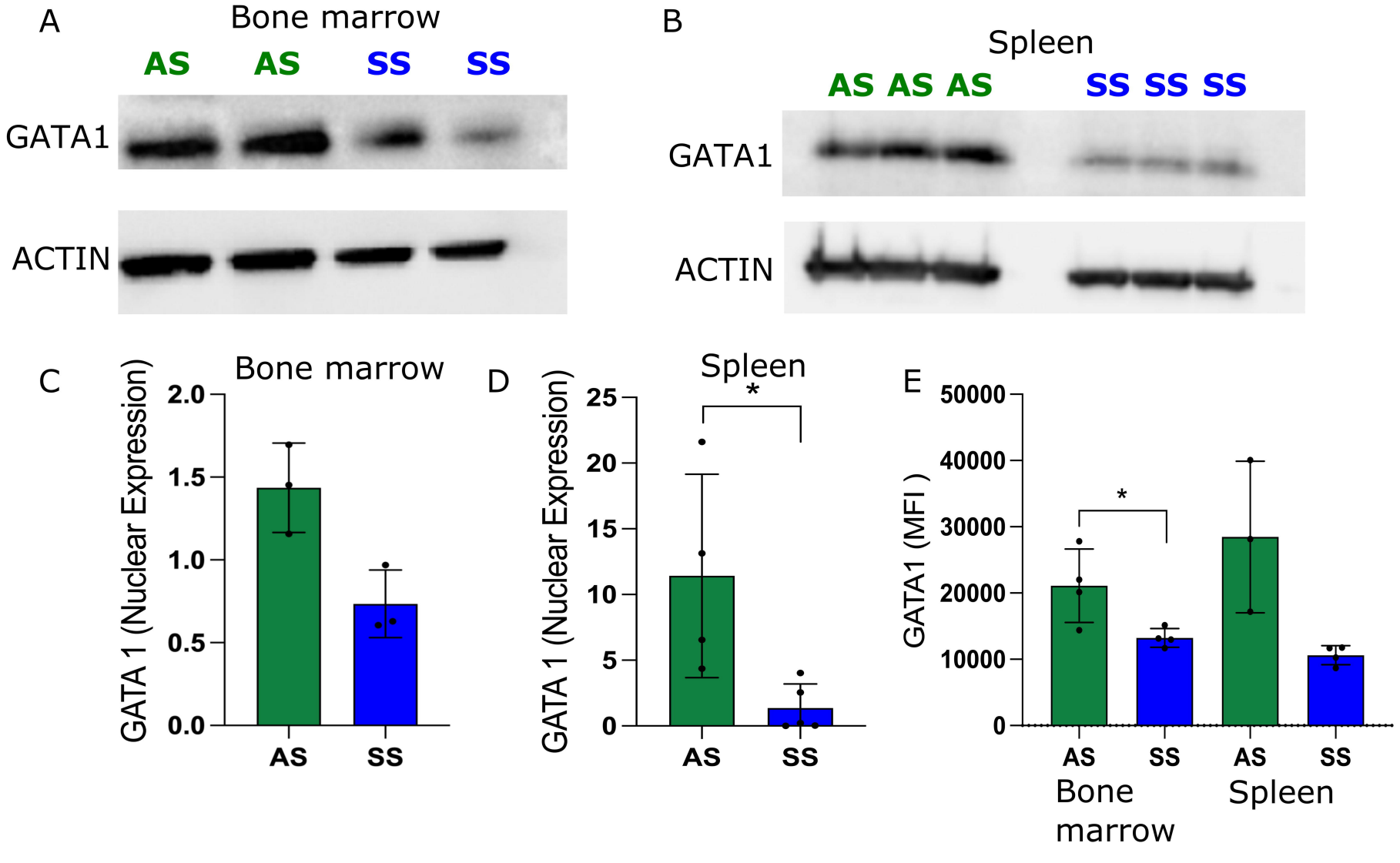
A
Bone marrow
AS AS SS SS
GATA1
ACTIN
B
Spleen
AS AS AS SS SS SS
GATA1
ACTIN
C
Bone marrow
GATA 1 (Nuclear Expression)
2.0
1.5
1.0
0.5
0.0
AS
SS
D
Spleen
*
GATA 1 (Nuclear Expression)
25
20
15
10
5
0
AS
SS
E
GATA1 (MFI)
50000
40000
30000
20000
10000
0
*
AS
SS
AS
SS
Bone marrow
Spleen

Figure 6

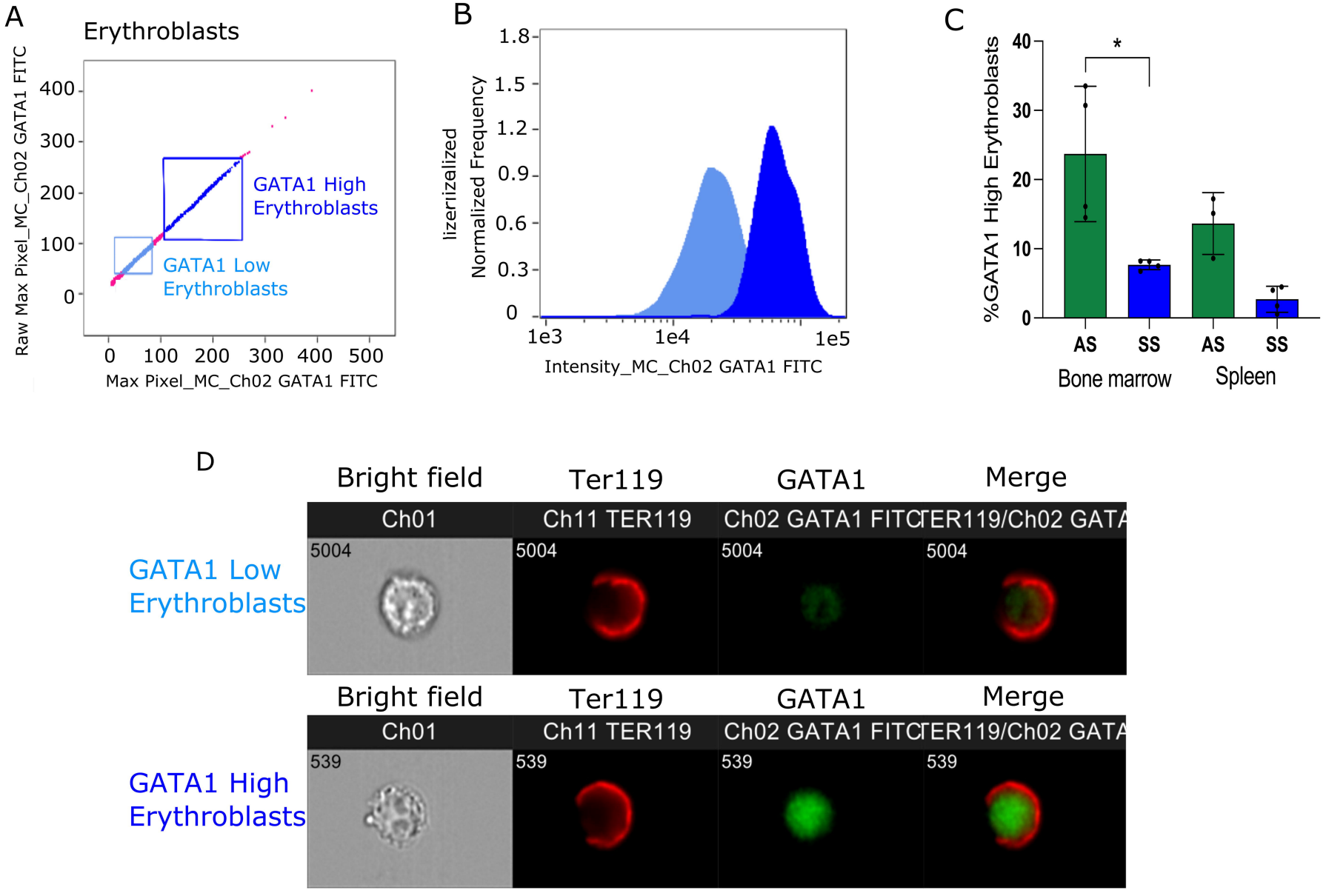
A
Erythroblasts
Raw Max Pixel_MC_Ch02 GATA1 FITC
Max Pixel_MC_Ch02 GATA1 FITC
GATA1 High Erythroblasts
GATA1 Low Erythroblasts
B
Normalized Frequency
Intensity_MC_Ch02 GATA1 FITC
C
%GATA1 High Erythroblasts
AS
SS
AS
SS
Bone marrow
Spleen
D
Bright field
Ter119
GATA1
Merge
Ch01
Ch11 TER119
Ch02 GATA1 FITC
TER119/Ch02 GATA
GATA1 Low Erythroblasts
GATA1 High Erythroblasts
5004
539

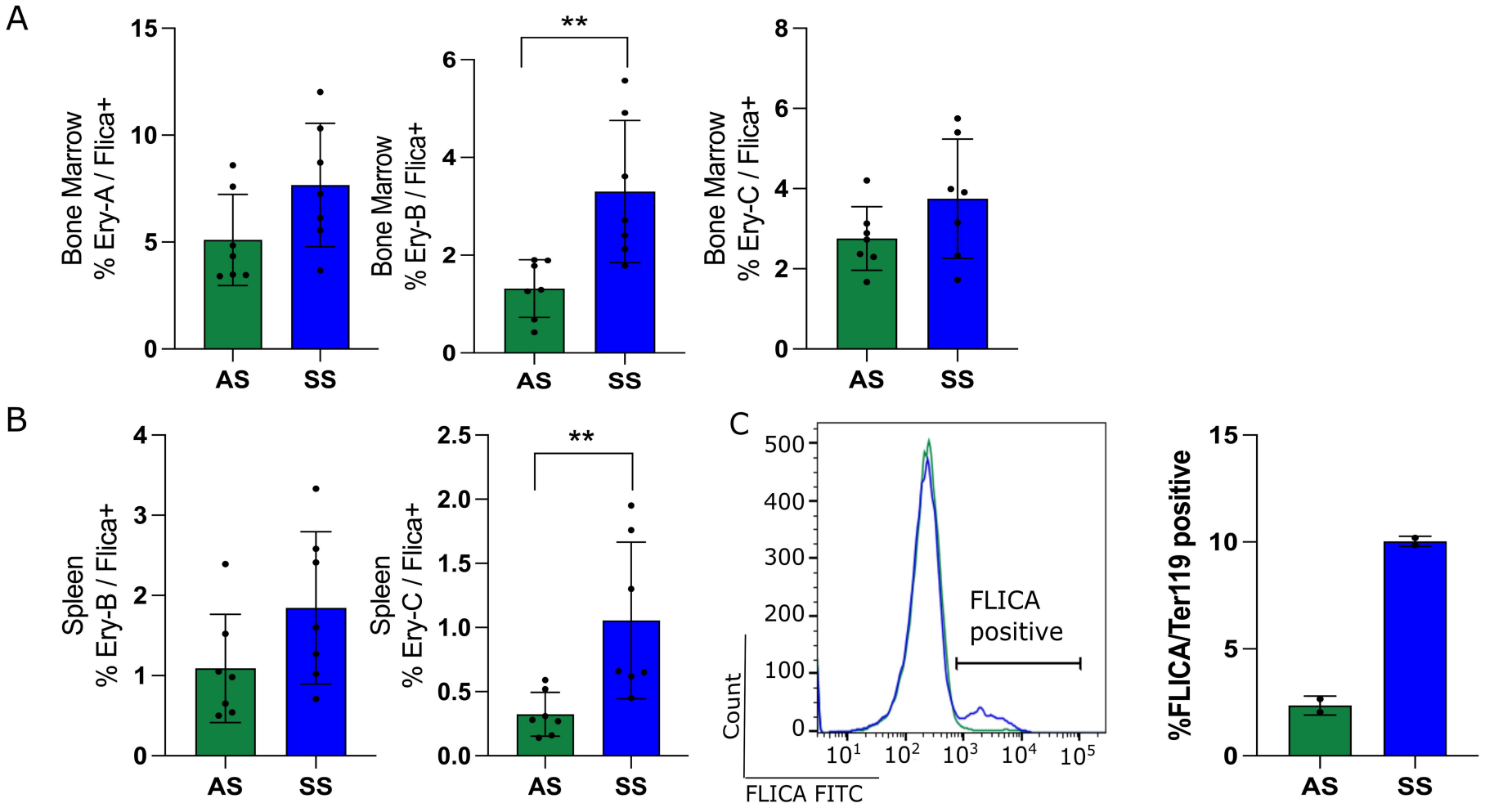
A
Bone Marrow
% Ery-A / Flica+
15
10
5
0
AS
SS
Bone Marrow
% Ery-B / Flica+
**
6
4
2
0
AS
SS
Bone Marrow
% Ery-C / Flica+
8
6
4
2
0
AS
SS
B
Spleen
% Ery-B / Flica+
4
3
2
1
0
AS
SS
Spleen
% Ery-C / Flica+
**
2.5
2.0
1.5
1.0
0.5
0.0
AS
SS
C
500
400
300
200
100
0
Count
FLICA
positive
10^1 10^2 10^3 10^4 10^5
FLICA FITC
%FLICA/Ter119 positive
15
10
5
0
AS
SS

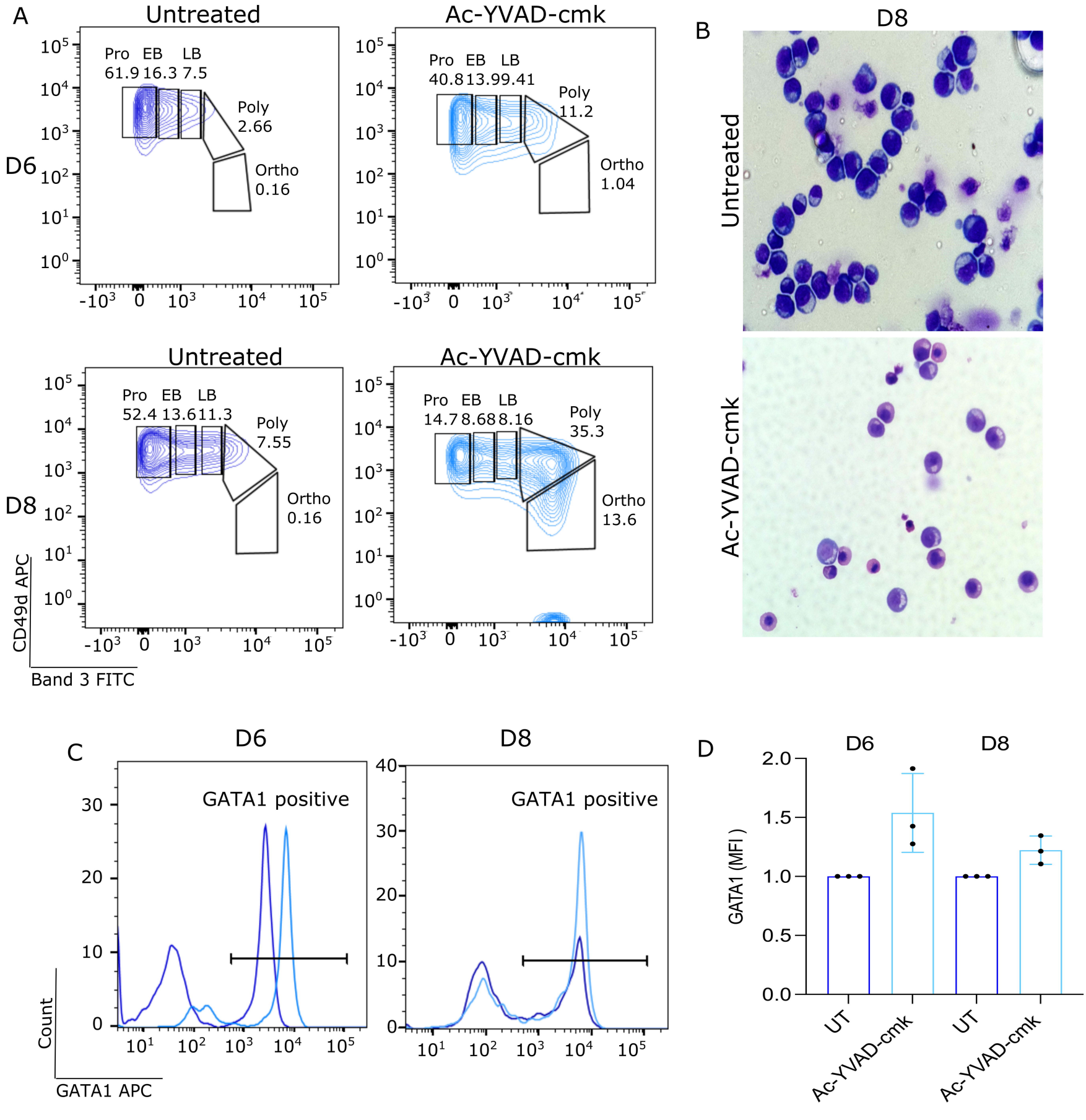
A
Untreated
Ac-YVAD-cmk
D6
Pro EB LB
61.9 16.3 7.5
Poly
2.66
Ortho
0.16
Pro EB LB
40.8 13.9 9.41
Poly
11.2
Ortho
1.04
D8
Pro EB LB
52.4 13.6 11.3
Poly
7.55
Ortho
0.16
Pro EB LB
14.7 8.68 8.16
Poly
35.3
Ortho
13.6
CD49d APC
Band 3 FITC
B
D8
Untreated
Ac-YVAD-cmk
C
D6
D8
GATA1 positive
GATA1 positive
Count
GATA1 APC
D
D6
D8
GATA1 (MFI)
UT
Ac-YVAD-cmk
UT
Ac-YVAD-cmk

Methods

Culture of HUDEP cells

Briefly, cells were maintained in expansion medium consisting of StemSpan SFEM (Stem Cell Technologies, catalog number:09650) supplemented with 50ng/mL Stem Cell Factor (SCF) (Peprotech, catalog number: 300-07), 3U/mL Erythropoietin (EPO) (NeoRecormon 2000U/0.3mL), 1µM dexamethasone (Sigma Aldrich, catalog number: D4902-100MG) and 1µg/mL doxycycline (Sigma Aldrich, catalog number: I2643-50MG). Cells were maintained at a concentration of 100,000 cells/mL. Differentiation was induced by seeding the cells at 2 x 10^5 cells/mL in differentiation medium containing 10ng/mL SCF, 1ng/mL Interleukin-3 (IL-3) (Stem Cell Technologies, catalog number: 78194.1), 3U/mL EPO, 1U/mL Penicillin – Streptomycin (Gibco, catalog number: 15140122) and 1µg/mL doxycycline. After day 2, cells were reseeded at 3.5 x 10^5cells/mL. After day 4 of differentiation, cells were reseeded at 5 x 10^5cells/mL without doxycycline. On day 8, cells were cultured in a differentiation medium containing holotransferrin (0.5mg/mL) (Sigma Aldrich, catalog number: T4132), 3U/mL EPO and 1U/mL Penicillin – Streptomycin and maintained at 1 x 10^6cells/mL with complete media change every other day.

Culture of $CD34^+$cells

Briefly, cells were cultured with 100ng/mL of Interleukin-6 (IL-6) (Miltenyi Biotech, catalog number: 130-093-929), 10ng/mL of IL-3 (Stem Cell Technologies, catalog number: 78194.1) and 50ng/mL of SCF (Peprotech, catalog number: 300-07) in a base medium composed of Iscove's Modified Dulbecco's Medium (IMDM) (Gibco, catalog number: 31980-048) supplemented with 15% BIT 9500 (Stem Cell Technologies, catalog number: 9500), 100 U/mL Penicillin Streptomycin (Gibco, catalog number: 15140122) and 2mM L-Glutamine (Gibco, catalog number: 25030-024). Medium was topped up every other day. After 9 days, the cells were cultured in the second phase medium containing 10ng/mL IL-3, 50ng/mL SCF and 2U/mL of EPO. Cells were maintained at a concentration of 200,000 cells/mL. Note that when appropriate, cultures were treated with Ac-YVAD-cmk, caspase 1 non-reversible inhibitor, at a concentration of 50µM (diluted in DMSO) at every media change during phase 2 of differentiation. Note that control condition was treated with similar volume of DMSO alone.

Antibodies

The antibodies used for the flow cytometry analysis are: BV421-conjugated anti-glycophorin A (GPA) (BD Bioscience), APC-conjugated anti-CD49d (BD Bioscience), FITC conjugated

anti-Band3 (Bristol Institute for Transfusion Sciences), AlexaFluor 647 anti-GATA1 (Cell Signaling). Cell stains 7-Aminoactinomycin D (7AAD) was purchased from BD Bioscience. For mouse experiments, APC anti-Ter119 and PE anti-CD71 were purchased from BD Bioscience.

The following antibodies were used for Western blot analysis: β-Actin Rabbit monoclonal antibody, FoxO3a Rabbit monoclonal antibody, GATA-1 (D24E4) Rabbit monoclonal antibody, NRF2 Rabbit monoclonal antibody. All antibodies were obtained from Cell Signaling. Anti-Rabbit IgG, HRP-linked secondary antibody was also obtained from Cell Signaling. Catalog numbers for all antibodies are listed in Supplementary Table 2.

Flow Cytometry

Differentiation Kinetics for human cells

The differentiation kinetics of CD34+ cells during phase 2 of culture were monitored every other day. Briefly, 10^5 cells were resuspended in 20µl of 1x PBS supplemented with 0.5% Bovine Serum Albumin (BSA) and incubated with GPA, CD49d and Band 3 (1/20 dilution) for 30 minutes in the dark. After two washes with 1x PBS /0.5% BSA, the cells were incubated with 7AAD for 5 minutes and analysed using the DIVA Software (version 9) on the FORTESSA Flow Cytometer (BD Bioscience). Compensation was performed using the BD Biosciences compensation beads, following the manufacturer instructions.

Reactive Oxygen Species (ROS) stain

The ROS Assay Kit 520nm (Invitrogen by Thermo Fisher Scientific, catalog number: 88-5930-74) was used according to the manufacturer's instructions. Briefly, 10^5 cells were stained for 60 minutes at 37^{o}C in 1x ROS Assay Stain diluted in ROS Assay Buffer. Cells were then analysed using the DIVA Software (version 9) on the FORTESSA Flow Cytometer (BD Bioscience).

GATA1 antibody staining

Cells (20^5) were stained with GPA for 30 minutes in the dark at 4^{o}C. Cells were then washed twice with 1xPBS 1/0.5% BSA. The Transcription Factor Buffer Set (BD Bioscience) was used to fix and permeabilize the nucleus prior to GATA1 staining, as per the manufacturer's instructions. Stained cells were incubated with 200µl of 1x Fix/Perm Buffer for 50 minutes at 4^{o}C, followed by 2 washes with 500µl of the 1x Perm/Wash Buffer. Cells were then stained with GATA1 (1 in 10 dilution) antibody for 50 minutes at 4^{o}C, followed by two washes with

1x Perm/Wash Buffer (cells were centrifuged at 400g for 6 minutes). Cells were analyzed using the DIVA Software (version 9) on the FORTESSA Flow Cytometry (BD Bioscience).

FAM-FLICA Caspase 1 Assay

Spleen and bone marrow cells ($1x10^6$ cells/tube in RPMI 1640; 100 µL) were used in assays. Antibody staining solution was prepared and added to each sample tube (1µL Ter119 PE, Invitrogen, Catalog number: 12-5921-83; 1µL CD71 PerCP-Cy5, BD Bioscience, Catalog number: 562858; 3.3 µL FAM-FLICA 30 x, ImmunoChemistry Technologies, Catalog number: FAM-FLICA Caspase 1 kit; 94.7 µL RPMI 1640 cell culture medium, Vitrocell, São Paulo, Brazil). Samples were incubated for 30 minutes, 37 °C. After the incubation, each sample was washed with 2 mL of 1x Apoptosis Wash Buffer and centrifuged at 200 x g, 5 minutes, 22°C. The samples were then fixed with 200 µL of FAM-FLICA fixing buffer (ratio of 1:5) and were immediately analyzed by FACS-Calibur flow cytometer (BD FACSCalibur™, BD Biosciences, Jan Jose, CA, USA), acquiring 10 000 events using the 488 nm laser. For analysis of FAM-FLICA, FlowJo VX software was used. Gating of erythroid progenitor cells for analysis by flow cytometry was performed as described by Shimet al. 2020[22]. The erythroid progenitor population is identified in mice as the CD71+Ter119+ population and includes the Pro E ($Ter119^{low}$) population and downstream progenitor populations. $Ter119^{high}$ cells were gated and differentiated by size into $Ter119^{+}CD71^{+}$ Ery A and Ery B. Ery C represents nucleated mature red blood cells (RBCs) that retain Ter119 but lose CD71 expression.

Microscopy

Cytospin was performed using 100,000 cells. Cells were washed twice with PBS and spun on slides using the Cytospin 2 centrifuge (Shandon). Slides were stained with May-Grunwald-Giemsa (MGG) stain following the manufacturer's instructions (Sigma). Slides were then washed with deionized water and left to dry. Slides were covered by a coverslip (Menzel – Glaser) Cells were imaged using an inverted microscope (Rebel by ECHO) at 20x and 40x magnification. Analysis was performed using the ImageJ software[34].

Protein extraction and western blot

Nuclear and cytoplasmic extracts were prepared from 3 x 10^6 cells using the NE-PER Nuclear and Cytoplasmic Extraction Reagents, according to the manufacturer's instruction (Thermo Scientific). 15µg of nuclear extract was analysed by SDS-PAGE using 10% polyacrylamide gels, followed by Western immunoblotting. Antibodies used include GATA1, FoxO3a,

NRF2and β-actin. Blots were developed using the Clarity and Clarity Max enhanced chemiluminescence (ECL) kits (Bio-Rad) and visualized on the Chemidoc MP imaging system (Bio-Rad). Analysis was performed using the Image Lab software (Bio-Rad). Antibodies are listed in the section above.

Isolation of murine bone marrow cells

Bone marrow cells were collected from euthanized AS and SS Berkeley mice under UK Home Office regulations. Bone marrow isolation was performed under sterile conditions. Bone marrow femurs were dissected, and the bone marrow was flushed out using an insulin syringe (INSU/LIGHT, #INS1ML27G13) and filter-sterile 1x PBS. Single-cell suspension was obtained by pipetting the bone marrow tissue up and down. The cell suspension was filtered through a 70μm cell strainer (BD Falcon).

Isolation of murine spleen cells

Each dissected spleen was placed in 3mL of 1x PBS and spun in the gentleMACS Dissociator (Miltenyi Biotec) which allows dissociation of tissues into a single-cell suspension. The cell suspension was passed through a 40μm Cell Strainer (BD Falcon) to ensure a single cell suspension.

Hemoglobin measurement in mice

Blood was drawn from mice under anesthesia using a syringe treated with heparin, and the samples were then placed into BD microtainer tubes with EDTA (Cat No 459036, Greiner Bio-one). The counts of red blood cells and hematocrit levels were assessed. Hemoglobin (Hb) concentrations were measured using the Hemocue Hb 201+ system. Comprehensive blood counts analyses for all samples were conducted at the Central Diagnostics Facility of the University of Cambridge.

Histology of bone marrow and spleen tissue

Bone marrow and spleen tissues from both treated and untreated animals were preserved using 10% formalin solution (Catalog Number P126-33 from Macron Fine Chemicals) and subsequently sent to Central Diagnostic Services, Queen's Vet School Hospital at the University of Cambridge. The long bone and muscle tissues underwent a decalcification process to eliminate calcium deposits. After decalcification, the tissues were embedded in paraffin wax. This included dehydration, clearing, and infiltration with wax to maintain the

structural integrity and preserve the microscopic details of the tissues. The embedded tissues were then thinly sliced and placed onto glass microscope slides. Finally, these sections were stained with Hematoxylin and Eosin (H&E)[35]. Images were taken using ECHO Rebel microscope.

Murine hematopoietic stem cell (HSC) isolation and *ex vivo* differentiation

Murine HSCs were isolated using the Lineage Cell Depletion Kit mouse (Miltenyi Biotec, catalog number: 130-090-858) and the MACS separator, following the manufacturer's instructions. Isolated HSCs were pelleted at 800g for 10 minutes at 4°C and resuspended in IMDM differentiation medium, supplemented with 20% FBS (Thermo Scientific, catalog number: 10270-106), 10 units/ml EPO (obtained from King's College Hospital Pharmacy, NeoRecormon 2000U/0.3mL) , 10 ng/ml SCF (Peprotech, catalog number: 300-07), 10 µM dexamethasone (Sigma Aldrich, catalog number: D4902-100MG), 100 ng/ml Insulin Growth Factor 1 (IGF1, R&D systems, catalog number: 791-MG), 2 mM L-glutamine (Gibco, catalog number: 25030081), 50 units/ml penicillin G and 50 µg/ml streptomycin (Sigma Aldrich, catalog number: P4333), 10^{-4}M β-mercaptoethanol (Sigma Aldrich, catalog number: M3148-25ML), 10 µg/ml recombinant human insulin (Merck #11061-68-0), 1% detoxified BSA (Sigma Aldrich, catalog number: 10735086001,), 200 µg/ml holotransferrin (Sigma Aldrich, catalog number: T4132) at a concentration of 0.1 x 10^6 / mL as described by (Shuga *et al.*, 2007). Differentiation kinetics were monitored by flow cytometry and microscopy as described herein.

Imaging Flow Cytometry staining in mice progenitor cells

Cells (50^5) were stained with Ter119 antibody for 30 minutes in the dark. Cells were then washed twice with 1x PBS/0.5% BSA. The Transcription Factor Buffer Set (BD Bioscience) was used to fix and permeabilize the nucleus prior to staining with GATA1 antibody, following manufacturer's instructions. Stained cells were incubated with 200µl of 1x Fix/Perm Buffer for 50 minutes at 4°C, followed by 2 washes with 500µl of the 1x Perm/Wash Buffer. Cells were then stained with GATA1 antibody (1/10 dilution) for 50 minutes at 4°C. After two washes with 500µl 1x Perm/Wash Buffer, the cells were processed using the INSPIRE software on the AMNIS Imagestream (Luminex). Analysis was performed using the IDEAS software (version 6.2). All analysis strategies are explained in Supplementary Figure 6.

Cell sorting of Ter119+ cells from the bone marrow and spleen of mice

Cells (10 million) were stained with Ter119 antibody for 30 minutes in the dark. Cells were then washed twice with 1x PBS/0.5% BSA. 4',6-diamidino-2-phenylindole (DAPI) was added as a dead/live stain. Cells were sorted into 15mL Falcon collection tubes containing 1mL of 1x PBS1/50%FBS, using the Aria cell sorter (BD Bioscience) with the collection chamber being at 4°C. The gating strategy for the sorting is explained in Supplementary Figure 5.

Cell staining for Cytof analysis

Cells (1.5 million) were thawed in IMDM medium and kept in the incubator at 37°C for one hour for recovery. Cells were then washed twice with Maxpar PBS (Standard Biotools) and centrifuged at 300g for 5 minutes. The cell pellet was then incubated with 2x Cell-ID Cisplatin-195Pt (Standard Biotools) for 5mins at 37°C. After incubation, cells were quenched and washed with Maxpar Cell Staining buffer (Standard Biotools) using 5x of packed cell volume, followed by centrifugation at 300g for 5 minutes. A blocking step was performed with 10µl of Human TruStain FcX (Standard Biotools) for 10minutes at room temperature and cells were pelleted. Antibodies against cell surface markers (Supplementary Table 1) were added to the cell pellet in 40µl of mastermix with antibodies added at a concentration of 1/100 to a total volume of 100µl), followed by incubation for 30 minutes at room temperature. Following the incubation, cells were washed twice with the Maxpar Cell Staining Buffer (Standard Biotools). For nuclear antibody staining, cells were permeabilized with 1mL of Maxpar Nuclear Antigen Staining Buffer (Standard Biotools), followed by incubation for 30 minutes at room temperature. Cells were then washed twice with 2mL of Maxpar Nuclear Antigen Staining Perm and centrifuged at 800g for 5 minutes. Antibodies against internal markers (Supplementary Table 1) were added to the cell pellet in 50µl of mastermix with antibodies added at a concentration of 1/100 in a total volume of 100µl, followed by incubation for 30 minutes at room temperature. This was followed by 2 washes (500µl) using the Maxpar Nuclear Antigen Staining Perm. A final incubation with the secondary antibodies was performed for 30 minutes at room temperature in a total volume of 100µl (50µl cell suspension and 50µl antibody mix). Cells were then washed with 2mL Nuclear Antigen Staining Perm buffer and centrifuged at 800g for 5 minutes. Cells were then fixed using 1.6% Formaldehyde (Sigma Aldrich). After fixation, cells were resuspended in 1mL intercalation solution and incubated overnight at 4°C. Cells were then analyzed on the Helios (A CyTOF System, Fluidigm). Analysis of data was performed using the OMIQ software.

Analysis of gene expression

Total RNA was extracted from 1 million erythroblasts using the RNeasy Midi Kit (Qiagen) following the manufacturer's protocol. First-strand cDNA was synthesized from 1 µg of total RNA with SuperScript III RNase H^- Reverse Transcriptase (Invitrogen) and oligo(dT)18 primer at 50°C for 50 minutes. Real-time PCR was performed using an ABI PRISM 7500 instrument (Applied Biosystems) with Power SYBR Green Master Mix. The reaction mixtures were incubated for 10 minutes at 95°C, followed by 40 cycles of 15 seconds at 95°C, 1 minute at 60°C, and a final step of 15 seconds at 95°C, 1 minute at 60°C, and 15 seconds at 95°C. Gene expression for each mRNA was normalized to PABPC1 in each sample.

Supplementary Figure Legends

Supplementary Figure 1: **Differentiation of WT and SS HUDEP-2**. (A) A contour plot of GPA+ cells from one WT (red) and one SS (blue) HUDEP-2 culture, showing the distribution of cell populations with respect to the expression of Band-3 FITC on the x-axis and CD49d-APC on the y-axis. Data are represented from day 0, 2, 4, 6 and 8 of differentiation. Pro: Proerythroblast, EB: Early Basophilic, LB: Late Basophilic, Poly: Polychromatic, Ortho: Orthochromatic erythroblasts. (B) Bar graph representing the percentage of proerythroblasts, early basophilic, late basophilic, polychromatic, and orthochromatic erythroblasts at day 2 of differentiation in WT (red) and SS (blue) HUDEP-2 cell line (n=4) (mean ± standard deviation). (C) Bar graph representing the percentage of polychromatic and orthochromatic erythroblasts at day 6 of differentiation in WT (red) and SS (blue) HUDEP-2 cell line (n=4). Images of WT and SS HUDEP-2 cells at (D) day 2 and (E) day 6 of differentiation, after MGG staining and visualization by light microscopy.

Supplementary Figure 2: **Schematic overview of the 2-step differentiation system of CD34+ hematopoietic stem and progenitor cells from sickle (SS) patients and healthy individuals and of the downstream analysis carried out at different stages of erythroid differentiation.**

Supplementary Figure 3: **Distribution of GPA in HD and SS differentiation.** (A) A line plot representation of the percentage of GPA positive cells observed during phase 2 of differentiation of CD34+ progenitor cells from one healthy donor (HD, red) and one SS patient (blue). (B) A bar graph showing the percentage of GPA positive cells at days 2, 4, 6 and 8 of phase 2 of differentiation of HD (red) and SS (blue) (n=4) (mean ± standard deviation). *$p<0.05$ Mann-Whitney test.

Supplementary Figure 4: **Erythroid differentiation of CD34+ cells isolated from the peripheral blood of Healthy donor (HD) and SS individuals.** (A) A contour plot of GPA+ cells from phase 2 of differentiation of one HD (red) and one SS (blue) CD34+ samples, showing the distribution of cell populations with respect to the expression of Band-3 FITC (x-axis) and CD49d-APC (y-axis). Data are presented for day 0 to day 12 of phase 2. Pro: Proerythroblast, EB: Early Basophilic, LB: Late Basophilic, Poly: Polychromatic, Ortho: Orthochromatic erythroblasts. (B) Bar graphs representing the percentage of proerythroblasts, early basophilic, late basophilic, polychromatic, and orthochromatic erythroblasts at day 2 (D2), day 4 (D4), day 6 (D6) and day 8 (D8) of differentiation (n=4) (mean ± standard

deviation). (C) Images of HD and SS cells stained with MGG at day 2, day 4, day 6 and day 8. *p<0.05, Mann-Whitney test.

Supplementary Figure 5: **Reactive oxygen species levels in WT and SS HUDEP-2 cell lines.** (A) Histogram showing reactive oxygen species (ROS) levels in WT (red) and SS (blue) HUDEP-2 cells on days 2 and 6 of differentiation. (B) Bar graph representing the fold change in mean fluorescence intensity (MFI) of ROS staining in WT and SS HUDEP-2 cell on days 2, 4, 6 and 8 of differentiation (n=4), (mean ± standard deviation).

Supplementary Figure 6: **mRNA levels of GATA1 in Healthy donor (HD) and SS individuals at day 6 of phase 2 of erythroid differentiation.** (n=4) (mean ± standard deviation).

Supplementary Figure 7: **GATA1 expression in WT and SS HUDEP-2 cell lines.** (A) Western blot images of GATA1 (upper panel) and Actin (lower panel) proteins in nuclear extracts from WT and SS HUDEP-2 cells on days 0, 2, 4 and 6 of differentiation. (B) Bar graph representing the quantification of GATA1 protein levels in the nuclear extracts of WT and SS HUDEP-2 cells on days 2 and 6, relative to Actin protein levels (n=3), (mean ± standard deviation).

Supplementary Figure 8: **A schematic representation of the experimental design for the AS and SS Berkeley mice.**

Supplementary Figure 9: **Histological analysis of the bone marrow and spleen of AS and SS Berkeley mice.** (A) Bar graph representing the hemoglobin (g/dL) levels in the peripheral blood of AS (n=5) and SS (n=8) mice. (B) A bar graph representing the animal weight (g) of AS (n=6) and SS (n=7) mice. (C) Left panel: An image showing the difference in size between AS and SS spleens; Right panel: bar graph representing the weight (g) of the AS (n=6) and SS (n=5) spleens. (D) Histopathology of bone marrow slices from AS (left) and SS (right) mice stained with HE. (E) Histopathology of spleen slices from AS (left) and SS (right) mice, stained with HE (upper panel) and Perls staining (stain of free iron deposit) (lower panel). *p<0.05, **p<0.01, ***p<0.001 Mann-Whitney test.

Supplementary Figure 10: **Erythropoiesis in the AS and SS Berkeley mice.** Density plot of Ery A (basophilic), Ery B (orthochromatic) and Ery C (reticulocytes) cell populations in the (A) bone marrow and (B) spleen of one AS and one SS mouse.

Supplementary Figure 11: **Flow cytometry gating strategy for the cell sorting of Ter119+ cells from the spleen and bone marrow of AS and SS mice**. The cells were first gated based on Forward Side Scatter – Area (FSC-A) and Side Scatter- Area (SSC-A). This was followed by single cell gating for gating and sorting Ter119+ cells using the FACS Aria 3 cell sorter (BD Bioscience).

Supplementary Figure 12: **Gating strategy for the GATA1 Low Erythroblasts and GATA1 High Erythroblasts using the IDEAS Software**. Cells were gated using the Aspect Ratio and Area features. Then the cells were gated based on focused images using the Gradient RMS feature. Focused cells were then gated based on Ter119 expression. An analysis mask was created next to distinguish between Ter119+ erythroblasts (with nucleus) and Ter119+ red cells (without nucleus). This was performed using the Perimeter and H-variance features of the cells.

The Erythroblasts were then used to create a new analytical pipeline that distinguishes the GATA1 Low Erythroblasts from the GATA1 High Erythroblasts, using the Max Pixel_MC_Ch02_GATA1.

Supplementary Figure 13: **Inhibition of caspase 1 activity.** (A) A bar graph representing GATA1 MFI level at day 6 in HD (red), SS (dark blue) and SS + Ac-YVAD-cmk (50µM) (light blue) erythroblasts. (n=3). (B) Bar graph representing MFI ROS levels in SS erythroblasts (dark blue) and SS+ Ac-YVAD-cmk (50µM) erythroblasts (light blue) at day 6 and 8 of differentiation (n=3).

Supplementary Tables

Supplementary Table 1: **Antibodies used for Cytof experiment.**

Product Name	Catalog Number	Surface / internal
Anti-human CD235a HIR2-141Pr	3141001B	Surface marker
Anti-Human CD117/c-kit (104D2)-143Nd	3143001B	Surface marker
Anti-Human CD34 (581)-148Nd	3148001B	Surface marker
Anti-Human CD36 (5-271)-155Gd	3155012B	Surface marker
Anti-Human CD49d (9F10)-174Yb	3174018B	Surface marker
Anti-Human CD71 (OKT-9)-175Lu	3175011B	Surface marker
Anti-PE (PE001)-156Gd	3156005B	Secondary antibody
Anti-APC (APC003)-176Yb	3176007B	Secondary antibody

Supplementary Table 2: **Antibodies used for western blot and flow cytometry.**

Product Name	Catalog Number	Manufacturer
BV421-conjugated anti-glycophorin A (GPA)	562938	BD Bioscience
APC-conjugated anti-CD49d	559881	BD Bioscience
FITC conjugated anti-Band3	5439FI	Bristol Institute for Transfusion Sciences
AlexaFluor 647 anti-GATA1	89084S	Cell Signaling
Cell stains 7-Aminoactinomycin D (7AAD)	559925	BD Bioscience
APC conjugated anti-Ter119	557909	BD Bioscience
PE conjugated anti-CD71	567206	BD Bioscience
β-Actin Rabbit monoclonal antibody	4970S	Cell Signaling
FoxO3a Rabbit monoclonal antibody	2497	Cell Signaling
GATA-1 (D24E4) Rabbit monoclonal antibody	4589S	Cell Signaling
NRF2 Rabbit monoclonal antibody	12721	Cell Signaling
Anti-Rabbit IgG, HRP-linked secondary antibody	7074	Cell Signaling

Supplementary Figure 1

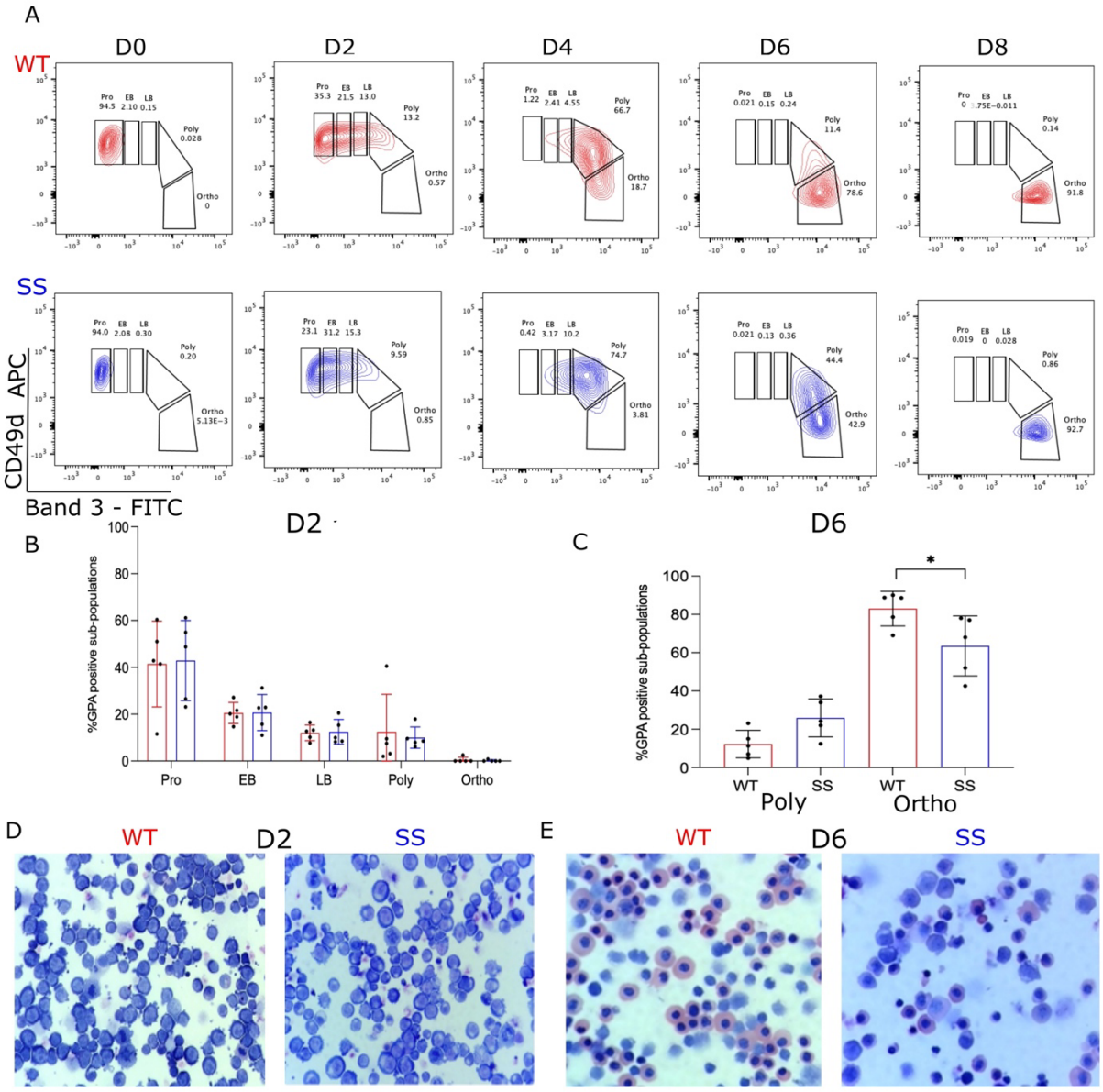

Supplementary Figure 2

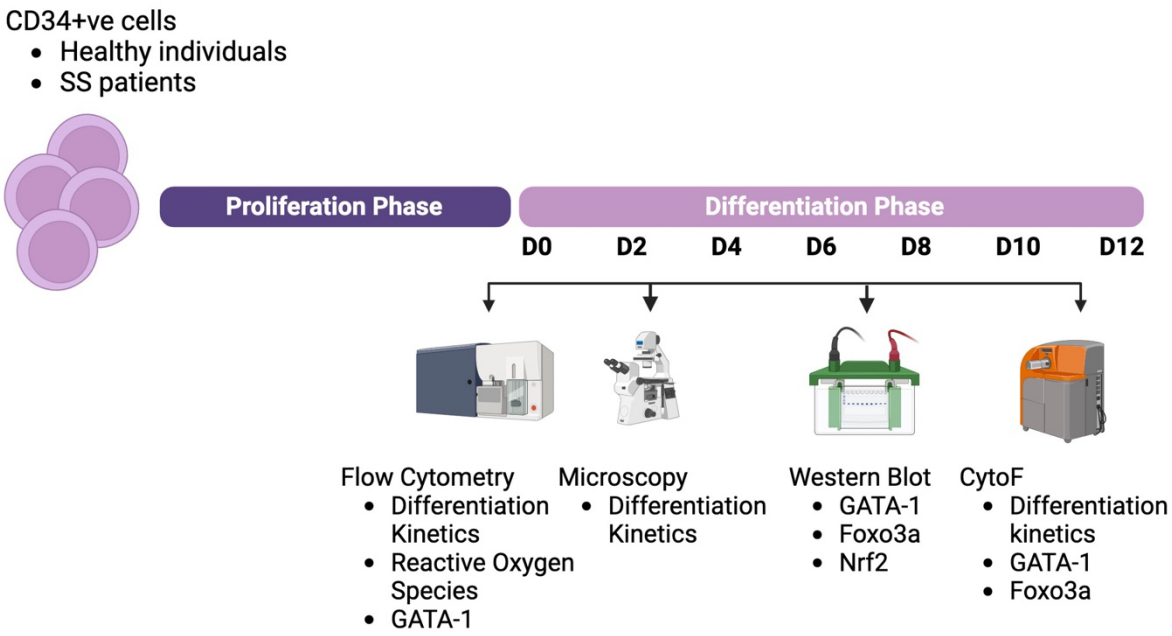

Supplementary Figure 3

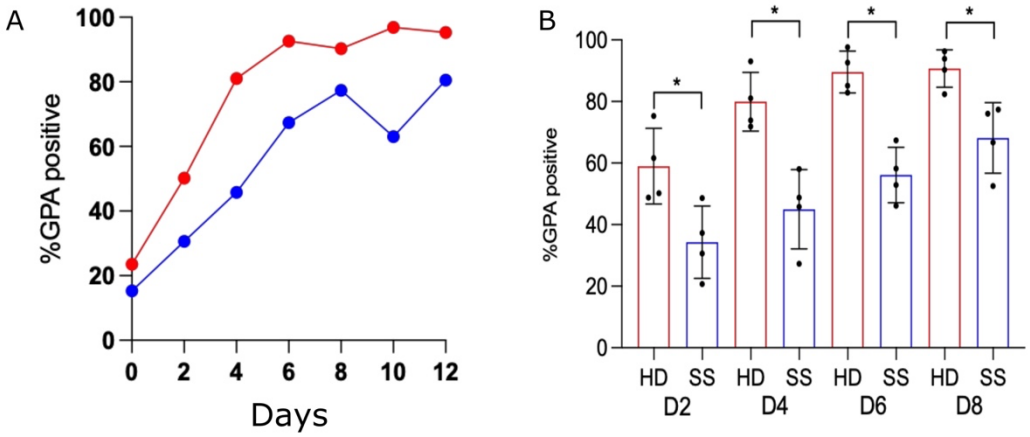

Supplementary Figure 4

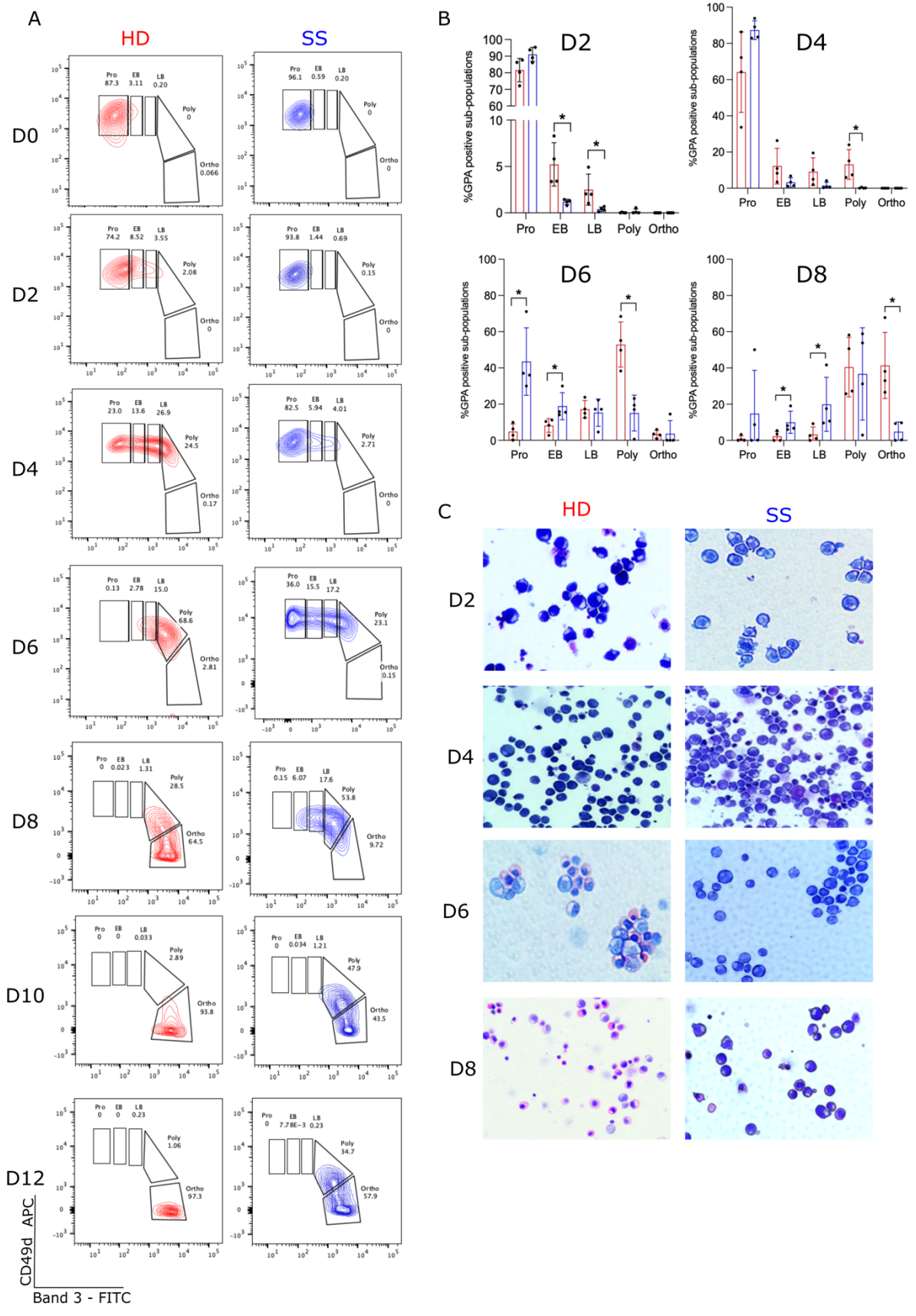

Supplementary Figure 5

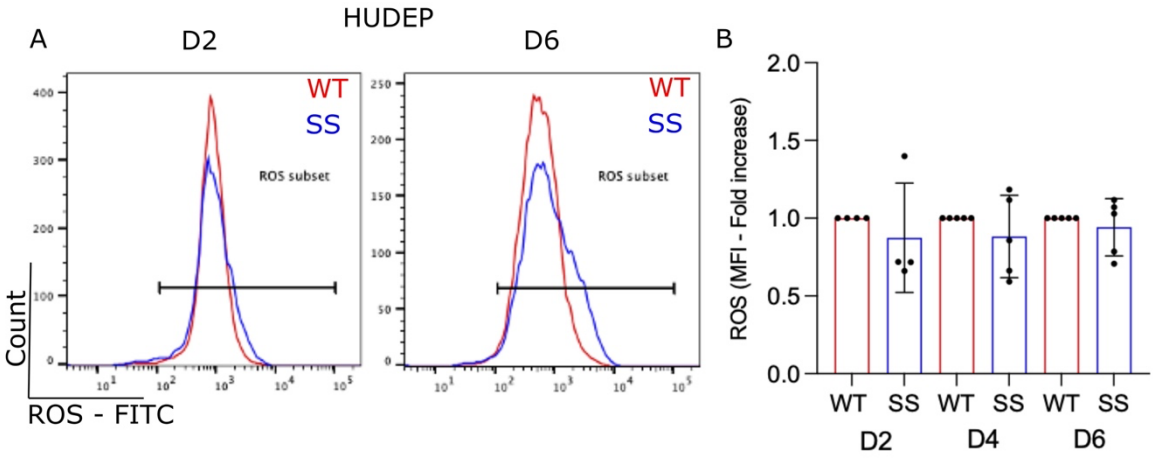

Supplementary Figure 6

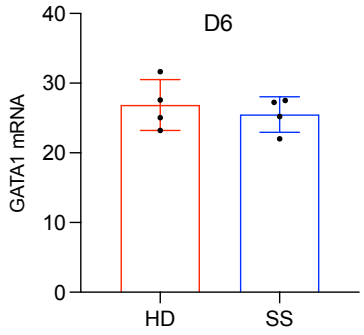

Supplementary Figure 7

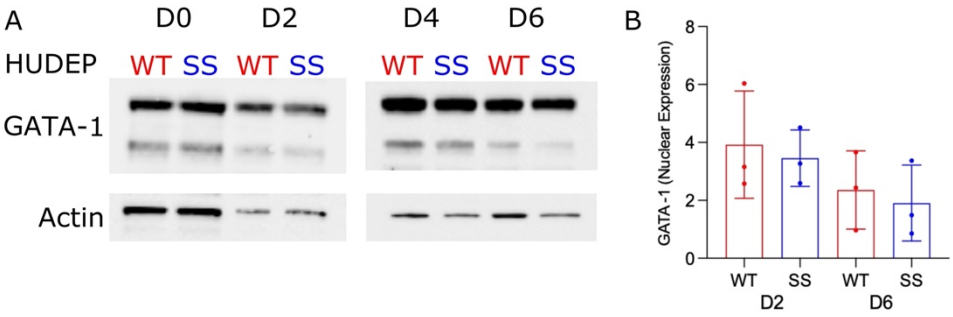

Supplementary Figure 8

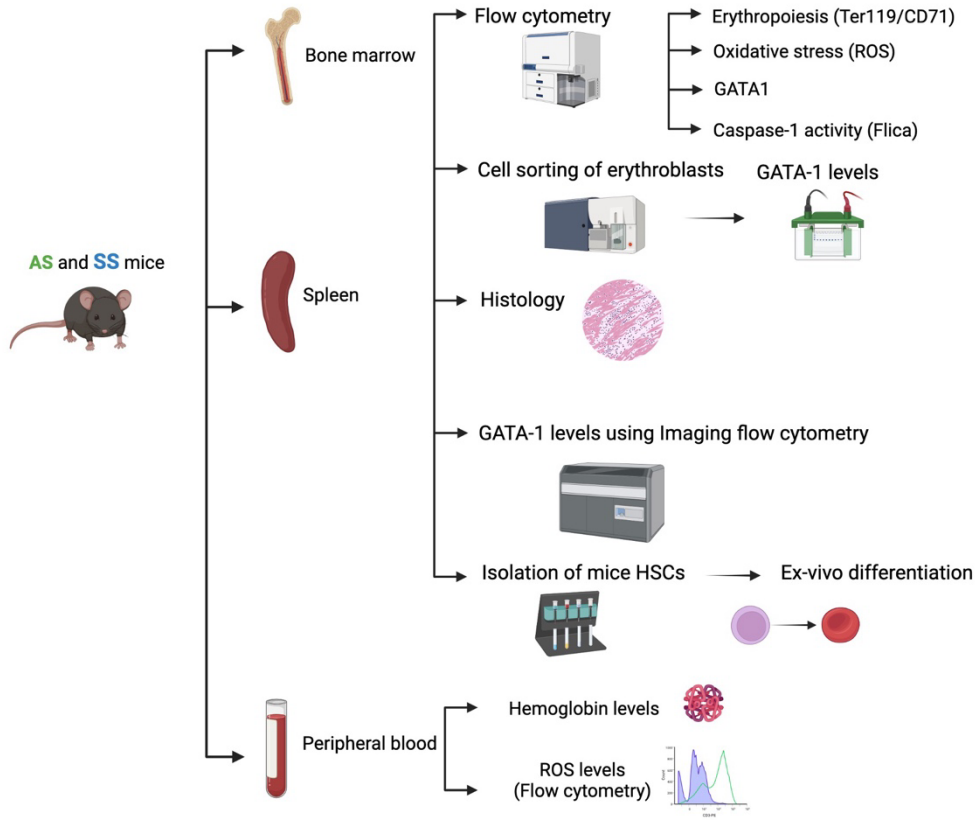

Supplementary Figure 9

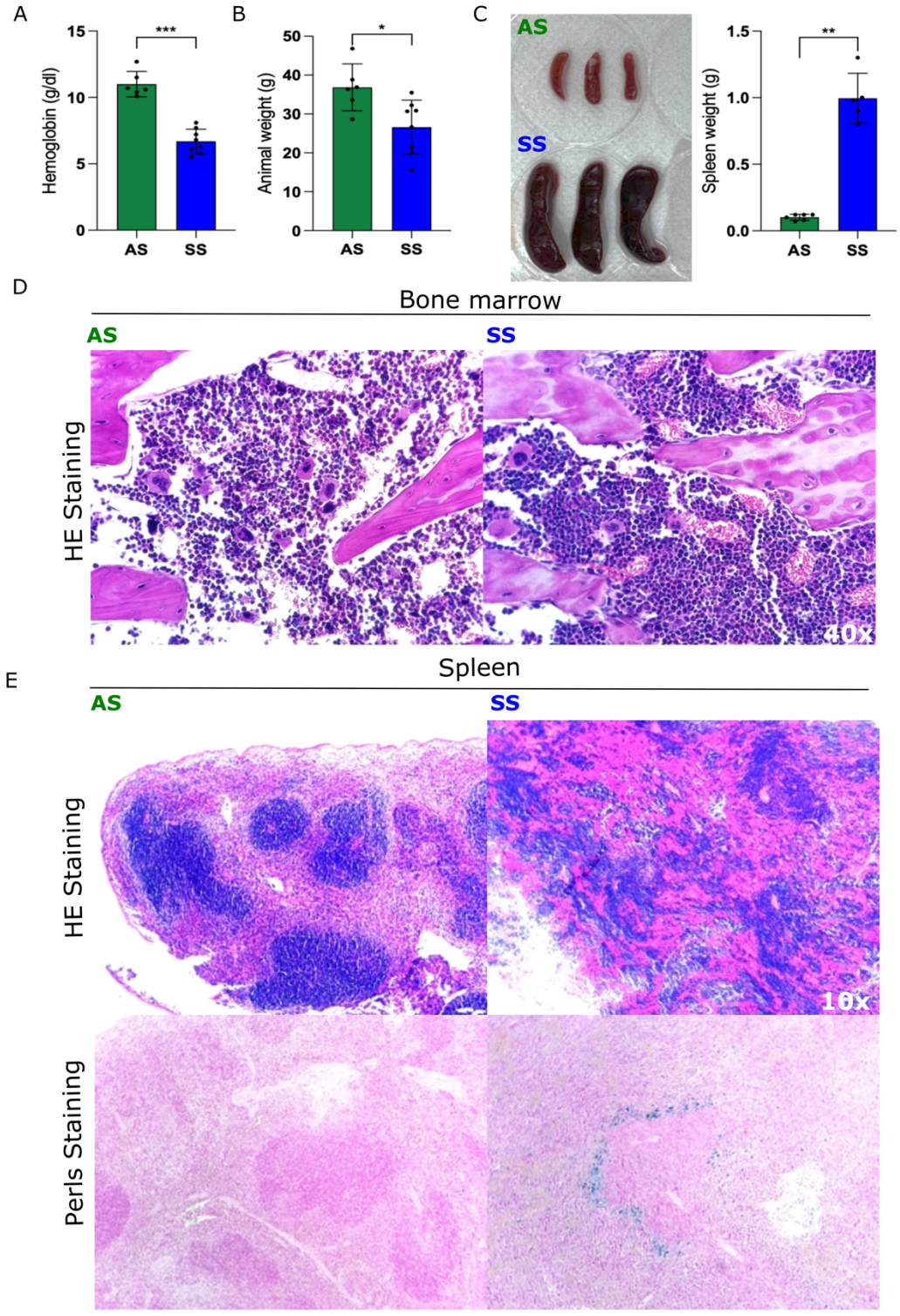

Supplementary Figure 10

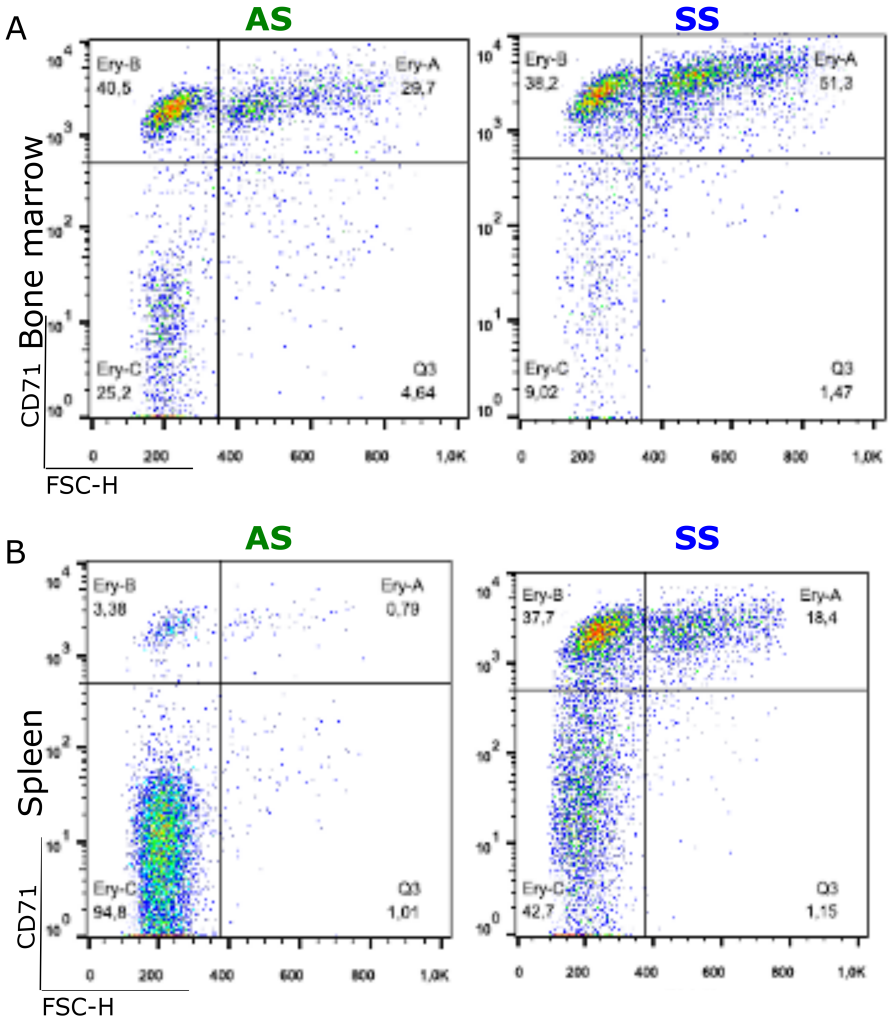

Supplementary Figure 11

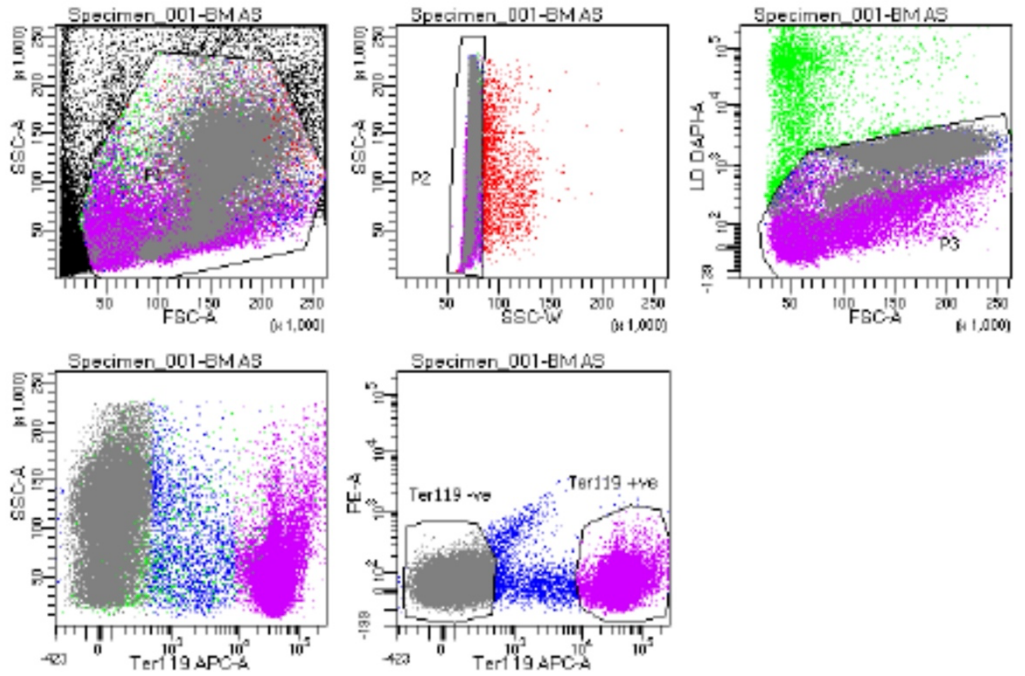

Sample	Ter119-	Ter119+
BM AS	4,003,986	4,145,218
BM SS	1,897,169	2,409,096

Tube: BM AS

Population	#Events	%Parent	%Total
All Events	75,746	####	100.0
P1	56,006	73.9	73.9
P2	54,139	96.7	71.5
P3	50,267	92.8	66.4
Ter119 +ve	23,645	47.0	31.2
Ter119 -ve	24,571	48.9	32.4

Supplementary Figure 12

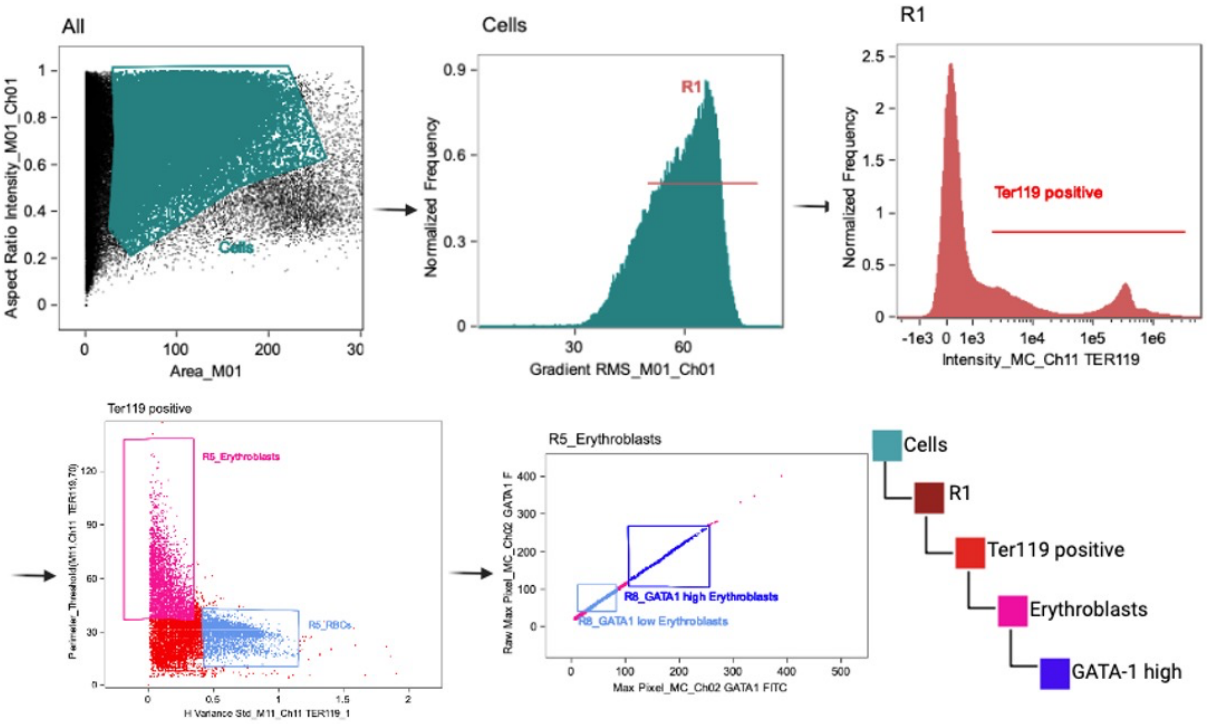

Supplementary Figure 13

A

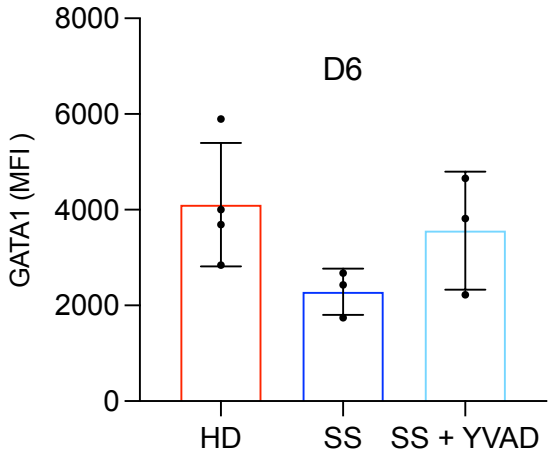

B